JAWRA Journal of the American Water Resources Association

RESEARCH ARTICLE

Benefits of Forests for Water: Projected Effects of Land Use Change in the San Jacinto Watershed, Texas

Sagarika Rath[1] | Peter Caldwell[2] | Sam Moore[1] | Patricia Spellman[3] | Raghavan Srinivasan[1] | Jeff Arnold[4] | Katie Martin[5] | Ge Sun[6] | Georgianne Moore[7] | James Vose[2]

[1]Texas A&M AgriLife Research, Blackland Research and Extension Center, Temple, Texas, USA | [2]Center for Integrated Forest Science, Southern Research Station, USDA Forest Service, Otto, North Carolina, USA | [3]School of Geosciences, University of South Florida, Tampa, Florida, USA | [4]USDA-ARS Grassland Soil and Water Research Laboratory, Temple, Texas, USA | [5]Department of Forestry and Environmental Resources, North Carolina State University, Raleigh, North Carolina, USA | [6]Eastern Forest Environmental Threat Assessment Center, Southern Research Station, USDA Forest Service, Otto, North Carolina, USA | [7]Department of Biology, Georgia Southern University, Statesboro, Georgia, USA

Correspondence: Sagarika Rath (sagarika.rath@ag.tamu.edu)

Received: 13 November 2024 | **Revised:** 2 October 2025 | **Accepted:** 7 January 2026

Keywords: land use projection | sediment yield | streamflow | SWAT | urbanization | water quality

ABSTRACT

Land use change poses challenges to water supply sustainability. The San Jacinto watershed located in Southeastern Texas is a microcosm of these challenges, with high dependence on surface water supply and projected urban and agricultural expansion by 2070, with a corresponding decline in forest and natural grassland. This study used the Soil and Water Assessment tool (SWAT) to evaluate the effects of these land use changes on water quality and quantity in the San Jacinto watershed. Our results indicated that projected land use change could increase annual average river discharge by as much as 6%, sediment load by ~40%, total nitrogen load by ~10% and total phosphorous load by ~20% across major tributaries within the watershed. We also show that current land use in 2020 may have increased the annual average sediment loads by 13%–80% and nutrient loads by 14%–40% relative to natural land uses (e.g., forests and grasslands), underscoring the sustainable clean water supply of natural land use types. Furthermore, while our model showed land use changes can cause high local variations in hydrological impacts, the overall effect at the watershed scale was lower, emphasizing the importance of focusing on sensitive local areas. This study provides a comprehensive and high-resolution assessment of the potential impacts of land use change on both water quantity and quality that can inform resource management decisions in a rapidly changing watershed.

1 | Introduction

Urban populations are expected to account for 66% of the global population by 2050 (UN DESA 2019; Salerno et al. 2018) and will significantly concentrate populations and increase demand for water, potentially stressing water availability. Urban expansion can exert substantial pressure on forests and other land uses, leading to deforestation, habitat fragmentation, and changes in agricultural practices (Brath et al. Brath et al. 2006; Zhang et al. 2018). Urban-induced alterations in flow dynamics and water quality have cascading effects on aquatic biodiversity, ecosystem health, and on downstream water supplies for human use. Therefore, a comprehensive understanding of the dynamic relationship between land use modifications and watershed hydrology is essential for sustainable land use planning, water resource management, and ecosystem preservation in swiftly urbanizing areas.

The transformation of land use and land cover (LULC) can have profound impacts on the natural hydrodynamics of watersheds by altering key processes such as runoff, infiltration, and evapotranspiration (ET) (Shi et al. 2007; Shrestha et al. 2018; Garg et al. 2019; Chilagane et al. 2021), impacting both water quantity and quality. For instance, the conversion of forested areas into

© 2026 American Water Resources Association. This article has been contributed to by U.S. Government employees and their work is in the public domain in the USA.

urban landscapes results in the proliferation of impervious surfaces such as roads and buildings, reducing the land's capacity for infiltration. Consequently, during extreme rainfall events, increasing stormwater runoff volumes may overwhelm drainage systems and heighten flood risk. This risk can be further exacerbated by climate change, as alterations in precipitation intensity and magnitude can amplify flood occurrences (Glick, Jeong, et al. 2023). In addition, runoff from impervious urban areas carries pollutants, including chemicals and sediments, worsening stream water quality and impacting downstream ecosystems (Callender and Rice 2000; Nelson and Booth 2002). Zampella et al. (2007) revealed that 10% or more of land use alteration for urbanization can result in significant changes in surface water quality.

When developing future watershed management plans for protecting water resources, it is imperative to understand the connections among LULC and water quality and quantity. Watershed models are widely used tools for studying hydrologic processes and their interactions with natural and human influences (Lirong and Jianyuna, Lirong and Jianyun 2012). Process-based models have proven instrumental in developing water management strategies, assessing reservoir sustainability, analyzing flood risk, and supporting sustainable land use planning (Tang et al. 2005). One widely used process model, the Soil and Water Assessment Tool (SWAT) has been successful for evaluating changes in water quality in response to LULC alterations and management practices (Ullrich and Volk 2009; Ghaffari et al. 2010; Bieger et al. 2015). SWAT has been used for urban and mixed-use watershed modeling (Dixon and Earls 2012; Eshtawi et al. 2016; Sisay et al. 2017) and is capable of simulating flashy urban storm runoff (Arnold et al. 2012; Jeong et al. 2010).

Southeastern Texas, which includes the city of Houston, USA, is at the crossroads of LULC change and climatological, ecological, and geomorphological gradients. Houston is one of the most populated urban areas of Texas with a metropolitan population of over 7 million as of 2022, which is estimated to reach nearly 10 million by mid-century (Greater Houston Partnership report (GHPR) 2023), while residential and vacant developable land has been projected to increase by 58% and decrease by 27% by 2040, respectively (Conlon et al. 2016; Houston-Galveston Area Council (H-GAC) 2020). The 2011 drought in the area was one of the worst and most persistent of its kind, while Hurricane Harvey in 2017 poured more than 50 in. of rain within a span of a couple of days, resulting in massive flooding. The San Jacinto watershed provides surface water supply for the city, primarily through drinking water intakes in Lake Conroe and downstream Lake Houston. The watershed provides water supply for the City of Houston, the regional water provider for approximately 2.2 million people in Harris County and portions of the three surrounding counties (https://www.houstonpublicworks.org/drinking-water-operations). The San Jacinto watershed is one of ten integrated water science basin studies identified by the USGS (Water Resource Mission Area, 2023) due to the water resource challenges arising from the large population centers that are impacted. The intersection of growing population and land use pressures, combined with large populations dependent on surface water for their drinking water supply, make the San Jacinto watershed an excellent case study to explore the potential impacts of land use change on water quantity and quality.

It is therefore imperative to comprehensively evaluate the effects of overall land use changes in Southeastern Texas as water resources are increasingly stressed. Previous studies using the SWAT model in Texas have highlighted various hydrological impacts of urbanization and land-use change in diverse watersheds. For instance, Jeong et al. (2010) evaluated urbanization impacts within the 369 km^2 Upper White Rock watershed, revealing significant shifts in flow and sediment due to urban growth. Zhao et al. (2016) extended this work to the much larger San Antonio watershed (10,826 km^2), where they noted heightened runoff and nutrient loads tied to urban development. Similarly, Pervaiz and Michelle A. H (2023) assessed 19 watersheds in Harris County, Texas, ranging from 39 km^2 to 1000 km^2, finding variable responses in flood risk and water quality depending on watershed size and urban extent. Shao et al. (2020) explored both the San Antonio watershed and the nearby Guadalupe River Basin (totaling 26,244 km^2), emphasizing differences in hydrologic behavior between these watersheds due to contrasting land uses and urban pressure. Lastly, Kim et al. (2016) analyzed the 720 km^2 Cypress Creek watershed, demonstrating the SWAT model's application to examine urban effects on hydrology within smaller subregions of the San Jacinto watershed; however, the impact of urban on sediment and nutrient load was not studied.

All of the past studies in the San Jacinto watershed have investigated how urbanization affects water resources in the city of Houston, but overlooked the broader implications of long-term overall land use changes (e.g., deforestation, agricultural and rangeland expansion) on hydrological processes and water quality across the entire watershed. To address these gaps in research, we conducted a detailed future land use study at a high resolution in the San Jacinto watershed. The primary objectives of this study were to quantify the effects of projected future land use changes on (1) water quantity and quality in major tributaries and water supply reservoirs within the watershed and (2) identify sensitive areas in the watershed that exhibit strong responses to land use change and impacts on water quality. Our results can then be used to better inform water resources management and help sustainable economic growth in the San Jacinto Watershed by minimizing and clearly understanding impacts on water quality and quantity.

2 | Methods

2.1 | Study Area

The San Jacinto River, located in southeastern Texas within the West Gulf Coast section of the coastal province (Figure 1), flows through a smooth, depositional plain that rises from sea level to an altitude of 153.7 m. Stretching 136 km, the river drains a land area of 7326 km^2 into Galveston Bay on the Gulf of Mexico. Two major tributaries feed the river: the East Fork and the West Fork. The West Fork flows into Lake Conroe and subsequently gathers water from Lake Creek, Spring Creek, and Cypress Creek before merging with the East Fork to form Lake Houston. Meanwhile, the East Fork combines with Peach Creek and Caney Creek on its way to Lake Houston. The climate is characterized as sub-humid with an average annual rainfall of 1330 mm and average annual maximum and minimum air temperatures of 26.3°C

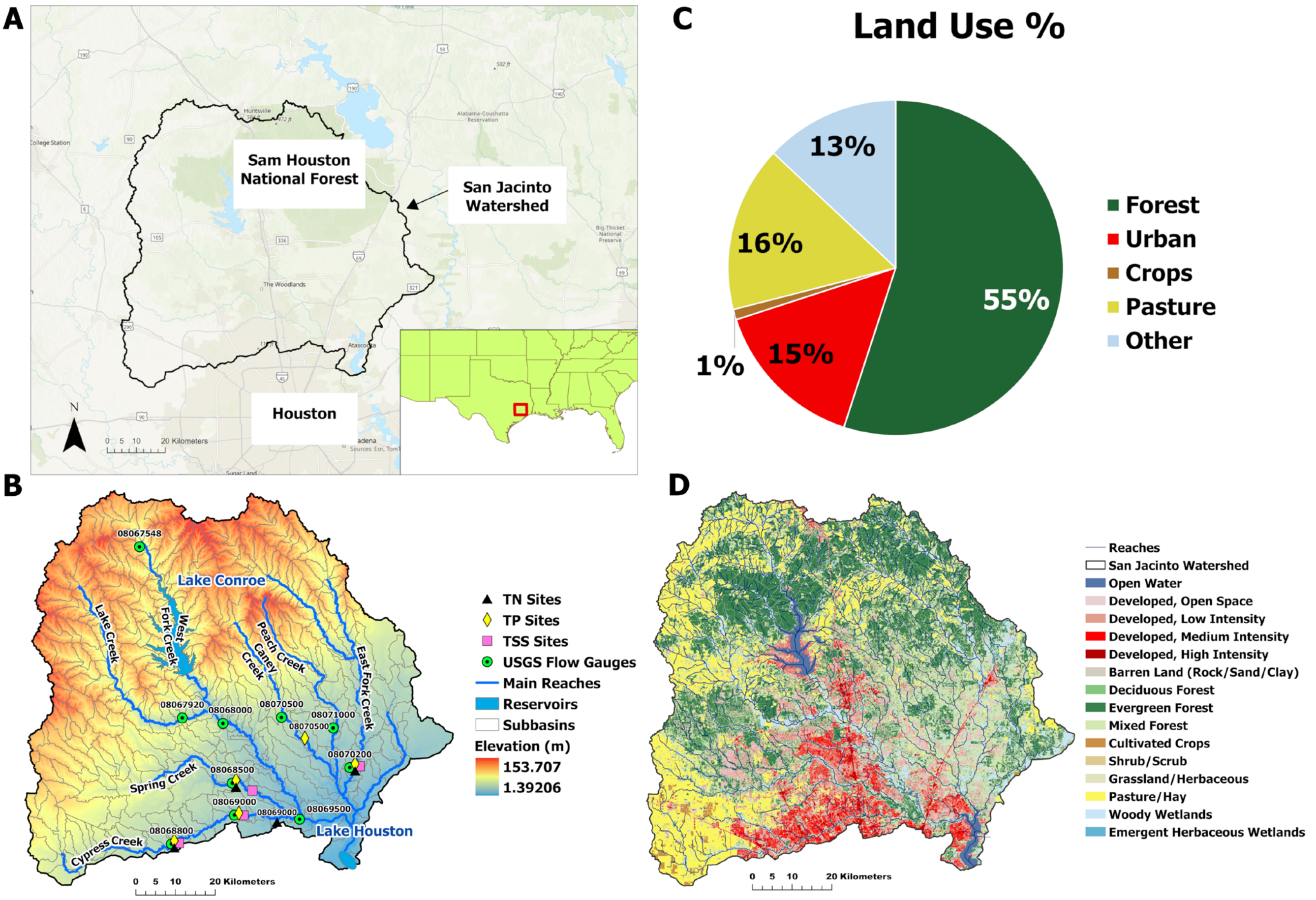

FIGURE 1 | Location of San Jacinto River basin in the United States and in southeastern Texas (A), The San Jacinto watershed boundary with elevation above mean sea level, location of reservoirs, gauges, and water quality monitoring sites (B), land use map for baseline model setup (modified 2016 NLCD (Homer et al. 2020)) based on 2020 RPA basemap (Langner et al. Langner et al. 2020) (C), and land use percentage of each land use (D). Forest includes NLCD classes Evergreen, Deciduous, and Mixed, developed includes classes High Intensity, Medium Intensity, and Low Intensity, and other land use class includes wetland, grass, scrub, barren land, and open water. The TSS site for Spring Creek is located at flow gauge site (08060550), to display clearly in the map it was shown with an offset.

and 13.5°C, respectively, obtained from 41 years of rainfall and temperature data spanning 1983–2023 (PRISM Climate Group 2023). More than 70% of annual rainfall occurs from May to December with drier periods from January to April (PRISM Climate Group 2023), and the eastern part of the watershed receives more rainfall than the western part (Figure S2). The San Jacinto watershed has had severe climatic events in recent years, including extended severe droughts in 2011 and 2012, as well as Hurricane Harvey in 2017.

Forest is the dominant land use in the watershed, followed closely by pastures and urban areas (Figure 1). Urbanization associated with Houston, Texas, occurs in the southwest portion of the watershed, with expansion to the south, west, and north (Kim et al. 2016). Between 1980 and 2012, the Houston metropolitan area experienced significant land cover change with urban expansion in all directions, particularly to the north, and a decrease in vegetated land (Brody et al. 2011; Zhu et al. 2015). Nearby watersheds, including Whiteoak Bayou, Buffalo Bayou, Brays Bayou, and Cypress Creek, experienced a 40% increase in developed land and a 20% to 60% decrease in grassland and agriculture after the 1990s (Zhu et al. 2015). Cypress Creek, part of the San Jacinto watershed, remains a less developed suburban area with about half of the area in developed land use and the other half a mix of forest, grassland, and agricultural ecosystems. The Cypress Creek watershed has experienced > 20% increase in developed land and reductions in forested areas (> 10%) and grassland (approximately 20%) between 1980 and 2015 (Zhu et al. 2015).

The area upstream of the Lake Conroe sub-watershed (1165 km^2) exhibits high forest land use occupied in part by the Sam Houston National Forest managed by the USDA Forest Service; however, the areas around the reservoir have undergone rapid urban development, and its location within the Houston metropolitan area has attracted heavy recreational use (San Jacinto River Authority 2015). Most of the water from the San Jacinto River and its tributaries is stored and managed in Lake Houston, operated by the City of Houston. Lake Conroe, co-owned by the San Jacinto River Authority (SJRA) and the City of Houston, is managed by SJRA. In Houston, about 95% of water is used for municipal and industrial purposes, with the remaining 5% used for irrigated agriculture. Ecological flows and freshwater inflows to Galveston Bay, essential for supporting fisheries and ecosystems, have become significant concerns in water resource management (Muttiah and Wurbs 2002).

2.2 | SWAT Model Overview and Setup

SWAT is a process-based, semi-distributed watershed scale simulation model developed by the United States Department of Agriculture-Agricultural Research Service (USDA-ARS) (Arnold et al. 2012). SWAT has been widely applied on various watersheds across diverse hydrological landscapes to simulate water quantity and quality, as well as to analyze the effects of land use change on water resource management (Schilling et al. 2008; Shi et al. 2011; Sajikumar and Remya 2015; Dogan and Karpuzcu 2022; Nepal and Parajuli 2024). SWAT discretizes a river basin into smaller sub-basins, and then each sub-basin is divided into hydrological response units (HRUs) defined as unique combinations of land use, soil, and topographic slope (Neitsch et al. 2005). Different hydrological components of the water balance including interception, surface runoff, percolation, ET, lateral flow through soil, groundwater flow (baseflow), soil moisture storage, and water yield (including both surface runoff and subsurface flows that ultimately contribute to streams) are computed at the HRU scale for a specified time step.

We used the Hydrologic and Water Quality System (HAWQS) (HAWQS 2020, https://epahawqs.tamu.edu/) (version 2.0) to streamline the San Jacinto SWAT model development to avoid the tedious initialization steps of preparing inputs required in the ArcSWAT platform and enabling faster model setup and execution (Yen et al. 2016). HAWQS is a web-based national-scale decision support tool developed by Texas A&M (n.d.) and supported by the EPA that integrates SWAT with high-resolution national datasets (Srinivasan 2019). It facilitates model setup, simulation, and output processing, with pre-loaded data at various spatial resolutions (Yen et al. 2016). HAWQS has been successfully used for various applications including predicting large-scale water quantity and quality in the Illinois River watershed (Yen et al. 2016), simulating future water quality conditions and economic impact in the United States (Fant et al. 2017), estimating ET in forest lands of Mississippi (Ouyang 2021; Chen et al. 2020), and assessing impacts of past hurricanes and tropical storms on hydrological processes in the Florida panhandle (Ouyang et al. 2022). These studies demonstrate the advantages of HAWQS as a time-saving and cost-effective modeling system when performing complex watershed simulations.

For this study, HAWQS was used to develop SWAT models for the San Jacinto watershed using the 14-digit Hydrology Unit Code (HUC 14) sub-basin boundaries and inputs from several well-established national datasets describing hydrology, land use, soils, crops, and weather (Table 1). Crop management information, such as planting, fertilizer application, and harvest data from the National Agricultural Statistics Survey (NASS) was assigned following the methodology outlined by White et al. (2016). No specific management operations were chosen for

TABLE 1 | List of model input data, source, and resolution. The details of data processing are available in https://hawqs.tamu.edu/content/docs/HAWQS_2.0_Technical_Documentation.pdf.

Data	Scale/extent	Source	References
DEM	10 m raster	National Elevation Dataset (NED), 2018 USGS	http://ned.usgs.gov/
Watershed boundaries	Average area of HUC14 is 22 km^2	National Hydrography Dataset Plus 2.0 (NHDPlus), HUCs14	https://www.epa.gov/waterdata/nhdplus-national-hydrography-dataset-plus
Land use/land cover used in HAWQs	30 m raster	National Agricultural Statistics Service (USDA-NASS n.d.) Cropland Data Layer, National Land Cover Database (NLCD n.d.)	USDA NASS CDL (n.d.)
Baseline (2020) and future (2070) land use/land cover used for future projections	90 m raster	USDA Forest Service 2020 Resources Planning Act (RPA), USDA Forest service 2023.	Homer et al. 2020, Brooks et al. 2023
Soil database	1:12,000 to 1:63,360 (30 m to 52 m)	Soil Survey Geographic Database (SSURGO) (USDA-NRCS).	USDA-NRCS (2019) http://soildatamart.nrcs.usda.gov
Point Source data	Within San Jacinto watershed	US EPA Hypoxia Task Force (HTF), Integrated Compliance Information System National Pollutant Discharge Elimination System (ICIS-NPDES).	EPA 2019. https://echo.epa.gov/trends/loading-tool/hypoxia-task-force-nutrient-model. USEPA 2009.
Reservoir operations	Lake Conroe	San Jacinto River Authority, National Inventory of Dams (NID).	Lee et al. (2012); San Jacinto River Authority (2020)
Weather (Precipitation, temperature)	Daily	PRISM (Parameter-elevation Regressions on Independent Slopes Model)	PCG 2019; USDA-NRCS 2019 https://prism.oregonstate.edu/
Measured streamflow	Daily	21 years of daily measured streamflow (2000–2020)	United States Geological Survey (USGS)
TSS and Nutrient data (TP and TN)	Discrete samplings	21 years of measured TSS and nutrient data at monthly interval (2000–2020)	Water Quality Portal (WQP) https://www.waterqualitydata.us/

forest lands, and the default option of natural forest growth was selected. Default pasture management of ungrazed managed pasture lands was considered for baseline model setup. Default SWAT parameters for pervious and impervious land management were assumed (Neitsch et al. 2011) for urban land uses including high intensity (70% impervious), medium intensity (48% impervious), and low intensity (12% impervious) land use. The previous portion of urban land use assumes managed grassland (lawn). Releases from Lake Conroe can influence downstream flow in West Fork Creek, which feeds into Lake Houston and impacts the overall water balance of the watershed. We accounted for the Lake Conroe dam by implementing reservoir parameters (Lee et al. 2012, San Jacinto River Authority 2020) in the SWAT setup. Since the Lake Houston reservoir is located at the watershed outlet, we treated the inflow to Lake Houston as the total water reaching the outlet and did not apply reservoir rules for Lake Houston, assuming it is undammed at the watershed outlet.

The point source data (Environmental Protection Agency (EPA) 2007) includes constant annual mean flows (cubic meters/day), total nitrogen (TN) (kg/day), total phosphorus (TP) (kg/day), and total suspended solids (TSS) loads (metric tons per day) for 453-point sources in the watershed (Figure S1) and were aggregated to the sub-basin level. All of these datasets, as well as the elevation and hydrology data, were preprocessed to increase the efficiency of the HAWQS model setup. The watershed was partitioned into 333 sub-basins based on the HUC 14 sub-basin boundaries (Figure 1). These sub-basins were further partitioned into 27,888 HRUs with similar land use, soil, and slope class.

2.3 | Calibration and Validation

Because nutrient and sediment load in channel strongly depend on streamflow (Pohlert et al. 2005; Ferrant et al. 2013; Epelde et al. 2016), a sequential method for model calibration was used by first calibrating the parameters influencing streamflow estimation, then TSS load, and lastly TP and TN loads (Santhi et al. 2001; Hundecha and Bárdossy 2004; Arnold et al. 2012). The SWAT model was calibrated for streamflow at 10 gauge sites in the watershed (Figure 1) operated and maintained by the United States Geological Survey (USGS) by using the Sequential Uncertainty Fitting Algorithm (SUFI2) with the SWAT Calibration Uncertainty Procedure (SWATCUP) (Abbaspour 2015; Abbaspour 2012). The model was executed using a 3-year warmup period (1997–1999) followed by calibration (2000–2014) and validation (2015–2020) periods.

The Load Estimator (LOADEST) (Runkel et al. 2004) was utilized to create a continuous monthly time series of observed TP, TN, and TSS loads from 2000 to 2020 at the monitoring sites for calibration and validation of model parameters. Recognizing the uncertainties associated with the LOADEST estimated load, the accuracy of modeled water quality parameters was further validated by comparing the calibrated nutrient load with monthly instantaneous measurements. SWAT parameters related to streamflow, sediment load, and nutrient loads (Tables S2 and S3) were selected from previous studies conducted in the San Jacinto watershed by (Lee et al. 2012; Kim et al. 2016; Sangeetha et al. 2022), expert judgments, and previous SWAT studies in similar hydrologic catchments in Texas (Saleh et al. 2000; Santhi et al. 2001).

Observed data for water quality were available at four monitoring sites for TSS and TP, and three monitoring sites for TN. Calibration and validation of TN were conducted for East Fork, Spring Creek, and Cypress Creek. The upstream TN monitoring site on Cypress Creek was used for calibration and validation, and results were evaluated at the downstream monitoring site (tx11324) using model-simulated flow due to the absence of observed flow data at that location. Due to varying land use patterns across the watershed (Figure 1), each tributary was individually calibrated for flow using the Kling-Gupta Efficiency (KGE) > 0.5 as the objective function. In addition, Nash Sutcliffe Efficiency (NSE) and percent bias (PBIAS) were considered to assess the model fit based on criteria established in Moriasi et al. (2015). The values of NSE and PBIAS were considered satisfactory for streamflow when NSE > 0.5 and PBIAS $< \pm 15\%$, for TSS when NSE > 0.45 and PBIAS $\leq \pm 20\%$, and for TN and TP when NSE > 0.35 and PBIAS $\leq \pm 30\%$ (Moriasi, Gitau, et al. 2015; Moriasi, Zeckoski, et al. 2015). With the final calibrated model parameters across the tributaries, the complete watershed model was run to check the sensitivity and the interaction of parameters among the sub-basins for streamflow, water quality, and the statistics of the objective function.

2.4 | Land Use Change Projections

We used land use projections developed as part of the USDA Forest Service 2020 Resources Planning Act (RPA) Assessment (USDA Forest service 2023) to assess how future land use change could impact flow and water quality across the San Jacinto watershed. The 2020 RPA projected land use from 2020 to 2070 on a decadal basis, focusing on the effects of socioeconomic and climatic changes across 20 combinations of four Shared Socioeconomic Pathways (SSPs) and five general circulation models (GCMs) (IPCC 2014). We selected two SSP scenarios among these (SSP3 and SSP5) to capture a range in projected population and economic growth assumptions coupled with two climate scenarios (HadGEM2-ES and MRI-CGCM3) that capture a range in potential future climatic conditions under the Representative Concentration Pathway (RCP) 8.5. SSP3 represents assumptions of relatively low GDP and population growth in the U.S., while SSP5 represents assumptions of relatively high U.S. GDP and population growth. Meanwhile, the HadGEM2-ES GCM (hereafter HAD) GCM was considered a "hot" climate scenario for the U.S., while the MRI-CGCM3 GCM (hereafter MRI) GCM was considered the "least warm" scenario (USDA, Forest Service 2023). Together, the two SSPs and two GCMs result in four future land use scenarios for this study: MRISSP3, MRISSP5, HADSSP3, and HADSSP5.

We used the 90 m gridded RPA land use projections for the 2020 basemap and 2070 projection from Brooks et al. (2023) for spatial realization. We disaggregated the broad land use classes used in the RPA assessment (water, developed, forest, other natural, pasture, and crop) into the narrower NLCD classes used by SWAT by overlaying the 2016 NLCD on the 2020 RPA basemap (the latter was derived from the 2016 NLCD) and assigning NLCD land cover classes to each 2020 RPA basemap pixel. These disaggregated land cover classes were retained for the future projections where no land use change was projected to occur. For pixels where land use change occurred in the future, we assumed that new development was NLCD class 22 (developed, low intensity, 12% imperviousness), new forest was NLCD class 43 (mixed forest), new pasture was NLCD class 81 (pasture/hay), and new crop was NLCD class 82 (cultivated crop).

The modified 2016 NLCD, which represents the 2020 RPA basemap, was used for baseline model setup for calibration. The calibrated model setup and historical weather period (2000–2020), referred to as the baseline model, was utilized for projected land use change analysis. Additionally, baseline point source inputs remained unchanged for all land use scenarios to isolate the effect of land use change on water quantity and quality compared to the baseline.

Two additional extreme scenarios of land use change were also explored to identify the potential envelope of hydrologic water quantity and quality response to land use change under (1) "Natural" land use: converting the urban land cover (originally 15% of the watershed) from the baseline model setup to evergreen forest, and transitioning pasture (originally 16%) and crop (originally 1%) areas to unmanaged grassland, while leaving other land uses unchanged, and (2) "Forest-to-Urban" land use: converting the baseline forest landcover (originally 55% of the watershed) to medium intensity urban landcover while converting pasture and crop to natural unmanaged grassland with the rest of the land uses remaining unaltered.

3 | Results

3.1 | Model Evaluation

3.1.1 | Streamflow

The calibration and validation statistics demonstrate the ability of the SWAT model to simulate streamflow, with "Satisfactory" to "Very Good" performance across calibration sites (Table 2; Figure 2; Figure S3). The "Good" statistics (NSE = 0.71, KGE = 0.78) at the gauge station downstream of Lake Conroe (USGS 08068000) indicated that the reservoir rules were effectively implemented in the SWAT model. Comparing our results with prior studies conducted in San Jacinto by Sangeetha et al. 2022 and Lee et al. 2012, our model output shows notable enhancements in performance. The model effectively captured the peak discharge events during the 2017 hurricane and the dry events in 2011 and 2012. All ten flow sites were rated from "Good" to "Very Good" for NSE at the monthly scale (Moriasi, Gitau, et al. 2015; Moriasi, Zeckoski, et al. 2015). More details regarding the adjusted parameters for calibration and parameter sensitivity for streamflow, TSS, TP, and TN, respectively can be found in Supplemental (Tables S1 and S2).

3.1.2 | TSS, TN and TP

Model performance metrics indicated TN, TP, and TSS at most sites were simulated within defined satisfactory ranges (Table 2; Figure 2; Figures S3 and S4). However, SWAT was unable to accurately capture peak TSS loads estimated by LOADEST during the validation period across all gauges (Figure 2 and Figure S4). These discrepancies could be attributed to measurement errors (Yen et al. 2015) and/or uncertainties in LOADEST estimation, which biases towards high flows (Park and Engel 2016; Singh et al. 2015). Additionally, possible alterations in forest land use management practices could lead to soil erosion that was not accounted for in the model setup. SWAT has limitations in predicting peak sediment loads, as it does not account for channel floodplain erosion during peak flows and relies on a simplified sediment routing process based on peak channel flow velocity (Benaman and Shoemaker 2005; Pai et al. 2011; Neitsch and Arnold 2001; Arnold and Srinivasan 1998). Despite challenges, SWAT demonstrated reasonable accuracy in predicting monthly TSS load, with all four sites rated as "Satisfactory" to "Very Good" for NSE and "Good" for PBIAS across the entire evaluation period. For TN and TP, model performance at the upstream Cypress Creek station (USGS 08068800) was "Unsatisfactory" for NSE during calibration, though PBIAS was "Very Good", while performance was "Satisfactory" for NSE and "Very Good" for PBIAS over the entire period. At the downstream Cypress Creek site (tx11334), NSE was "Satisfactory," and PBIAS was "Very Good" in both calibration and validation periods. Across all TN sites, performance ranged from "Satisfactory" to "Good" for NSE and "Very Good" for PBIAS.

3.2 | Baseline Conditions

3.2.1 | Water Quantity and Quality

Water quantity and quality varied spatially throughout the watershed as a function of land use. The model estimated watershed-wide water balance under baseline model setup is typical of the region (Table 3) and suggests a high degree of spatial variability in water balance components (ET, percolation, and water yield) across sub-basins according to land use distribution (Figures 1 and 3). The simulated watershed average annual evapotranspiration and water yield were 855 mm and 326 mm, respectively, accounting for 64% and 25% of the average annual precipitation (1325 mm), comparable with long-term annual budgets reported in previous studies (Lee et al. 2012; Reitz, Sanford, et al. 2017; Reitz, Senay, and Sanford 2017; Sangeetha et al. 2022; Wurbs 2021).

Regionally, the urban-dominated sub-basins of Cypress Creek had the highest mean annual water yield (550–750 mm) and the lowest ET (approximately 600 mm) and percolation (50–150 mm). In contrast, forest-dominated areas such as East Fork Creek, upstream of Lake Conroe, and upstream of Spring Creek had relatively higher percolation (250–350 mm), ET (over 800 mm), and lower water yield (< 350 mm). The extreme west region of the watershed generated relatively higher baseflow (150–200 mm) due to prominent shrublands, wetlands, and grasslands, which enhanced percolation. This regional variability reflected land use influences (Figure 4), with natural grasslands contributing approximately 550 mm of water yield per year through baseflow (approximately 250 mm), urban areas contributing approximately 450 mm of water yield primarily through surface runoff, and forests showing the lowest water yield

TABLE 2 | Monthly statistics for flow, TSS, TP, and TN over calibration, validation, and entire period. The NSE and PBIAS were assigned a parameter-specific performance rating (superscript notes) according to Moriasi et al. (2007, 2012, 2015), where VG = Very Good, G = Good, S = Satisfactory, and US = Unsatisfactory.

	Calibration (2000–2014)				Validation (2015–2020)				Entire period (2000–2020)			
Gauging site	**NSE**	**R^2**	**PBIAS (%)**	**KGE**	**NSE**	**R^2**	**PBIAS (%)**	**KGE**	**NSE**	**R^2**	**PBIAS (%)**	**KGE**
Flow (cumecs)												
Lake Conroe (USGS 08067548)*	0.60^{S}	0.61^{S}	24.20^{S}	0.61	0.95^{VG}	0.91^{VG}	12.6^{G}	0.87	0.9^{VG}	0.91^{VG}	−22.6^{S}	0.77
DS Lake Conroe (USGS 08068000)	0.64^{S}	0.64^{S}	−1.40^{VG}	0.76	0.73^{G}	0.74^{G}	−8.60^{VG}	0.76	0.71^{G}	0.71^{G}	−4.7^{VG}	0.78
Lake Ck (USGS 08067920)[a]					0.96^{VG}	0.95^{VG}	−11.1^{G}	0.88	0.96^{VG}	0.95^{VG}	−11.1^{G}	0.88
Spring Ck (USGS 08068500)	0.69^{G}	0.70^{G}	8.90^{VG}	0.80	0.94^{VG}	0.94^{VG}	−11.70^{G}	0.88	0.86^{VG}	0.86^{VG}	0.6^{VG}	0.92
Cypress Ck (USGS 08068800)	0.77^{VG}	0.81^{VG}	12.80^{G}	0.82	0.67^{G}	0.91^{VG}	−11.80^{G}	0.54	0.72^{G}	0.87^{VG}	1.9^{VG}	0.68
Cypress Ck (USGS 08069000)	0.71^{VG}	0.77^{VG}	−20.40^{S}	0.60	0.79^{VG}	0.83^{VG}	−15.40^{G}	0.68	0.77^{VG}	0.81^{VG}	−18.40^{S}	0.65
Upstream to Lake Houston West Fork Ck (USGS 08069500)[a]					0.83^{VG}	0.88^{VG}	21.7^{S}	0.72	0.83^{VG}	0.88^{VG}	21.7^{S}	0.72
East Fork Ck (USGS 08070200)		0.77^{VG}	−8.80^{VG}	0.76	0.87^{VG}	0.90^{VG}	−4.10^{VG}	0.76	0.83^{VG}	0.83^{VG}	−6.8^{VG}	0.84
Caney Ck (USGS 08070500)	0.54^{S}	0.58^{S}	8.40^{VG}	0.74	0.89^{VG}	0.94^{VG}	−7.0^{VG}	0.81	0.74^{G}	0.78^{VG}	2.5^{VG}	0.85
Peach Ck (USGS 08071000)	0.59^{S}	0.64^{S}	27.60^{US}	0.64	0.91^{VG}	0.92^{VG}	18.10^{S}	0.80	0.81^{VG}	0.83^{VG}	23^{S}	0.73
TSS Load (Tons)												
Spring Ck (USGS 08068500)	0.65^{S}	0.70^{G}	-45^{S}	0.52	0.68^{G}	0.84^{VG}	−0.40^{VG}	0.50	0.68^{G}	0.76^{G}	−20^{G}	0.52
Cypress Ck (USGS 08068800)	0.72^{G}	0.79^{G}	−17.30^{G}	0.75	0.73^{G}	0.92^{VG}	−22.0^{G}	0.56	0.75^{VG}	0.89^{VG}	−15.6^{G}	0.66
Cypress Ck (USGS 08069000)	0.59^{S}	0.59^{S}	3.80^{VG}	0.71	0.50^{S}	0.84^{VG}	−32.0^{US}	0.27	0.50^{S}	0.61^{S}	−17.7^{S}	0.50
East Fork Ck (USGS 08070200)	0.47^{S}	0.72^{G}	35.3^{US}	0.28	0.67^{G}	0.76^{G}	−30.10^{US}	0.49	0.67^{G}	0.68^{G}	7.0^{VG}	0.66
TP Load (kg)												
Spring Ck (USGS 08068500)	0.61^{G}	0.63^{S}	−11.1^{VG}	0.74	0.57^{G}	0.66^{G}	13.6^{VG}	0.47	0.59^{G}	0.63^{G}	1.3^{VG}	0.55
Cypress Ck (USGS 08068800)	0.76^{VG}	0.77^{G}	−2.5^{VG}	0.85	0.87^{VG}	0.92^{VG}	11.30^{VG}	0.84	0.84^{VG}	0.86^{VG}	−2.9^{VG}	0.91
Cypress Ck (USGS 08069000)	0.52^{G}	0.64^{S}	−20.00^{S}	0.58	0.73^{G}	0.89^{VG}	−23.90^{S}	0.63	0.66^{VG}	0.76^{G}	−23.30^{S}	0.61
East Fork Ck (USGS 08070200)	0.61^{G}	0.64^{S}	−24.3^{S}	0.62	0.70^{VG}	0.93^{VG}	−46.4^{US}	0.39	0.70^{VG}	0.84^{VG}	−36^{US}	0.49
TN Load (Kg)												
Spring Ck (USGS 08068500)	0.57^{S}	0.64^{G}	−17.30^{VG}	0.73	0.66^{G}	0.69	−14.10^{VG}	0.71	0.67^{G}	0.7^{G}	−15.6^{VG}	0.73
Cypress Ck (USGS 08068800)	0.18^{US}	0.50^{S}	7.50^{VG}	0.54	0.40^{S}	0.68	41^{US}	0.47	0.36^{S}	0.59^{S}	19.40^{VG}	0.56
Cypress Ck (tx11334)	0.46^{S}	0.62^{G}	4.90^{VG}	0.71	0.43^{S}	0.61	0.7^{VG}	0.7	0.46^{S}	0.62^{G}	3.3^{VG}	0.72
East Fork Ck (USGS 08070200)	0.54^{S}	0.64^{G}	9.70^{VG}	0.76	0.67^{G}	0.67^{G}	7.30^{VG}	0.71	0.62^{G}	0.64^{G}	8.70^{VG}	0.77

*Denotes the calibration data available from 2010.
[a]Denotes data available for validation period.

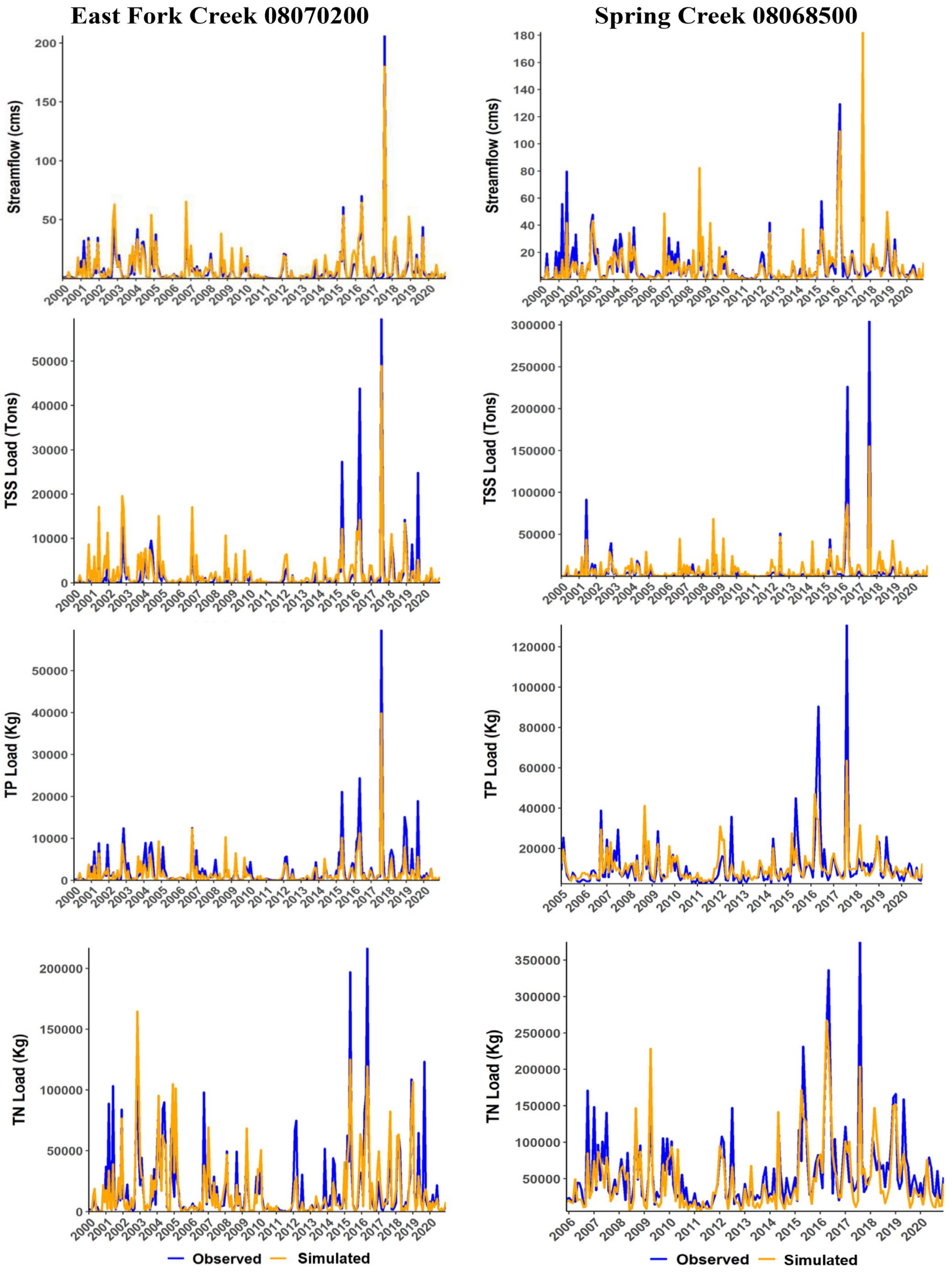

FIGURE 2 | Legend on next page.

FIGURE 2 | Simulated and observed monthly flow, TSS, TN, and TP for example sites East Fork Creek Gauge site (08070200) and Spring Creek Gauge Site (08068500). TP observed data available beginning in 2005 and TN data available beginning in 2006 for Spring Creek. Please refer to Figures S3 and S4 for the rest of the calibration sites.

TABLE 3 | Percent differences in annual average water balance of watershed for all projected and extreme scenarios in comparison to baseline, and absolute value of simulated annual average (2000–2020) water balance components for baseline shown in second column. Precipitation (PCP) was 1325 mm across the watershed for all scenarios.

Variable	Baseline (mean annual) units (mm)	Values in % difference from baseline					
		MRI SSP3	MRI SSP5	HAD SSP3	HAD SSP5	Natural	Forest-to-Urban
ET	855	−1.15	−1.12	−1.04	−1.04	−4.09	−15.25
Percolation	218.21	1.59	1.42	1.65	1.54	21.95	−26.42
Water yield	326.27	2.71	2.71	2.37	2.43	5.56	53.39
Surface runoff	232.26	3.05	3.14	2.56	2.68	−5.39	84.59
Lateral flow	10.67	−0.19	−0.28	0.00	−0.09	7.59	−25.87
Baseflow	79.94	2.04	1.80	1.06	1.97	37.48	−21.73
ET/PCP	0.64	0.64	0.64	0.64	0.64	0.62	0.55
Water yield/PCP	0.25	0.25	0.25	0.25	0.25	0.26	0.38

(approximately 300 mm) and surface runoff (approximately 150 mm). Forest and grassland land use also exhibited higher percolation rates (approximately 250 mm and 450 mm, respectively), highlighting their groundwater recharge potential.

The annual average sediment, TP, and TN yields across the sub-basins in the watershed also varied with land use (Figure 3). Those sub-basins in the highly urbanized Cypress Creek sub-watershed had among the highest predicted yields, with more than 2 tons/ha/yr of sediment, approximately 2 kg/ha/yr of TP, and more than 10 kg/ha/yr of TN. Figure 4 shows croplands produced relatively higher median sediment yield (2.5 tons/ha/yr) and TN (10 kg/ha/yr) compared to other land uses due to management practices and application of fertilizer on crops. In contrast, forest, grassland, and pasture land uses generated lower median sediment yields (0.5 tons/ha/yr), TN yields (0.5 kg/ha/yr for forest and grassland, and 2.5 kg/ha/yr for pasture), and TP yields (0.1 kg/ha/yr for forest, grassland, and 0.6 kg/ha/yr for pasture) (Figure 4). Mean sediment yields from forest land and grassland were approximately 100% lower than crop land and approximately 75% lower than urban land.

3.3 | Conditions Under Land Use Projections

Land use projections for the San Jacinto watershed indicate a continued shift of pasture, grassland, and forest, with increased urbanization and agricultural expansion by 2070. Urban area is expected to rise from 15% in 2020 to 20%, while forest area may decrease from 55% to 51%. Although cropland comprised only 1% of the watershed in 2020, it is predicted to more than double in some scenarios by 2070. Detailed land use changes across tributary sub-watersheds are highlighted in the Supporting Information (Table S3, Figure 5). At the tributary sub-watershed level, cropland is projected to increase 60%–70% in the Lake Conroe watershed, over 200% in East Fork Creek, and 96%–294% in Spring Creek. Although these percentages indicate substantial growth, the actual cropland area remains relatively modest, as cropland constitutes a small portion of the overall watershed. In Cypress Creek, cropland is projected to grow from 42 to 120 km^2 (over 150%) under MRI SSP3 and SSP5, with more modest increases of 30%–33% (42 to 57 km^2) under HAD SSP3 and SSP5 scenarios.

3.3.1 | Land Use Change Effects on the Water Balance

Future land use projection scenarios resulted in modest changes to overall watershed-wide water balance components such as ET, water yield, and percolation (Table 3), but larger changes were projected at the sub-basin and sub-watershed scale. Model results projected a watershed-wide decline in ET (up to 1.17%), increase in water yield (up to 2.57%), and increase in surface runoff (up to 3.05%) (Table 3), with the MRISSP5 scenario having the most impact due to a larger reduction in forest land (248 km^2) and greater urban expansion (375 km^2) (Table S3).

Compared to ET (Figure 6A) and water yield (Figure 6C), projected changes in percolation had greater spatial variation across the watershed (Figure 6B) due to heterogeneity in soil properties, with 60% of the watershed projected to experience increased percolation. Larger decreases (> 10%) were projected in the lower portion of the watershed, particularly in East Fork Creek, where urban land use increased by over 200% (Figure 5). Larger percolation increases (> 10%) were projected in the northwestern portion of the watershed, including upstream

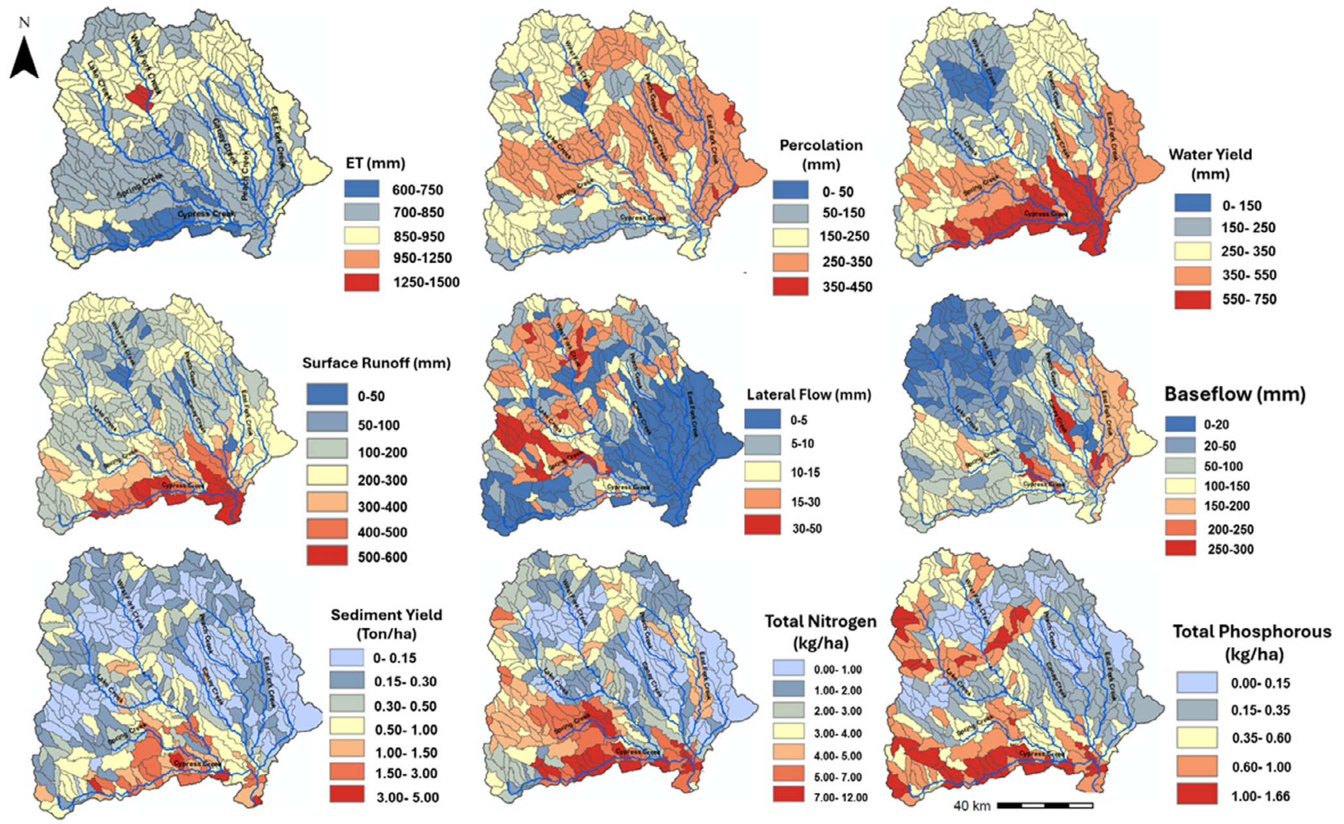

FIGURE 3 | Spatial distribution of annual average (2000–2020) water balance components, sediment, total phosphorus and total nitrogen yield across sub-basins.

sub-basins of Lake Conroe, due to a 38–48 km^2 expansion of grass/shrubland replacing pasture and forest land. Upstream Cypress Creek sub-basins showed 2.5%–10% increases in percolation due to pasture-to-cropland conversion. While percolation rates were similar between cropland and pasture (Figure 4), variations arise from soil types and crop management. Thus, conversion from pasture to crop can result in increases in percolation and water yield under certain conditions.

The spatial pattern of water yield changes mirrored that of ET, with water yield increasing where ET decreased and vice versa. ET was projected to decrease up to 25% for 80%–87% of the watershed under future land use, with greater reductions (> 10%) upstream of Lake Conroe and Lake Creek due to urban land replacing pasture and forest land. An estimated 80% of the watershed was projected to experience a water yield increase (up to 25%) across scenarios, with 42%–45% of the watershed projected to experience minimal changes (±1%), 42%–47% moderate changes (±1%–5%), and 7%–10% over 5%–10% increases (Figure 6C). Larger projected increases in water yield occurred in the northern upstream areas and Cypress Creek, while East Fork showed a 2.5%–5% increase in water yield but over a 25% rise in surface runoff due to an increase in impervious surfaces.

“Natural” and “Forest-to-Urban scenarios” allowed us to identify the potential envelope of hydrologic response to land use change. Under the “Natural” scenario, watershed-wide percolation increased by 21.95%, ET decreased by 4.09%, and water yield increased by 5.56% (Table 3). These changes suggest that while converting urban areas to forests may increase ET and reduce water yield, the conversion of pasture and cropland (18% of the watershed) to grassland can offset this effect by decreasing ET and increasing water yield. Baseflow and lateral flow increased substantially in the “Natural” scenario by 37.48% and 7.59%, respectively, while surface runoff decreased by 5.39%. Conversely, the “Forest-to-Urban” scenario resulted in a 26.42% decline in percolation, a 15.25% decrease in ET, and a 53.39% increase in water yield (Table 3). Surface runoff increased by 84.59% under this scenario, while baseflow decreased by 21.73% due to reduced percolation. In the “Natural” scenario, water yield declined by up to 25% in upstream sub-basins of Lake Houston (Figure S5) due to reduced surface runoff, while increasing in the Lake Conroe and upstream Cypress Creek sub-basins. In contrast, water yield was projected to increase in all sub-basins under the “Forest-to-Urban” scenario, with Lake Conroe, Caney Creek, and Lake Creek exceeding 100% increases in water yield.

3.3.2 | Land Use Change Effects on Streamflow

The average annual streamflow was projected to increase by 1%–5.6% across all four land use scenarios (Figure 7) for selected reaches, with the largest projected increase at Lake Conroe (4.5%–5.8%), compared to Lake Houston (2% to 2.5%) and other tributaries. The MRISSP3 and MRISSP5 scenarios consistently projected higher streamflow increases across all reaches, while HADSSP3 had a lesser impact, except at Lake Conroe. East Fork and Spring Creek showed less than a 2% increase in annual average flow, whereas the more urbanized

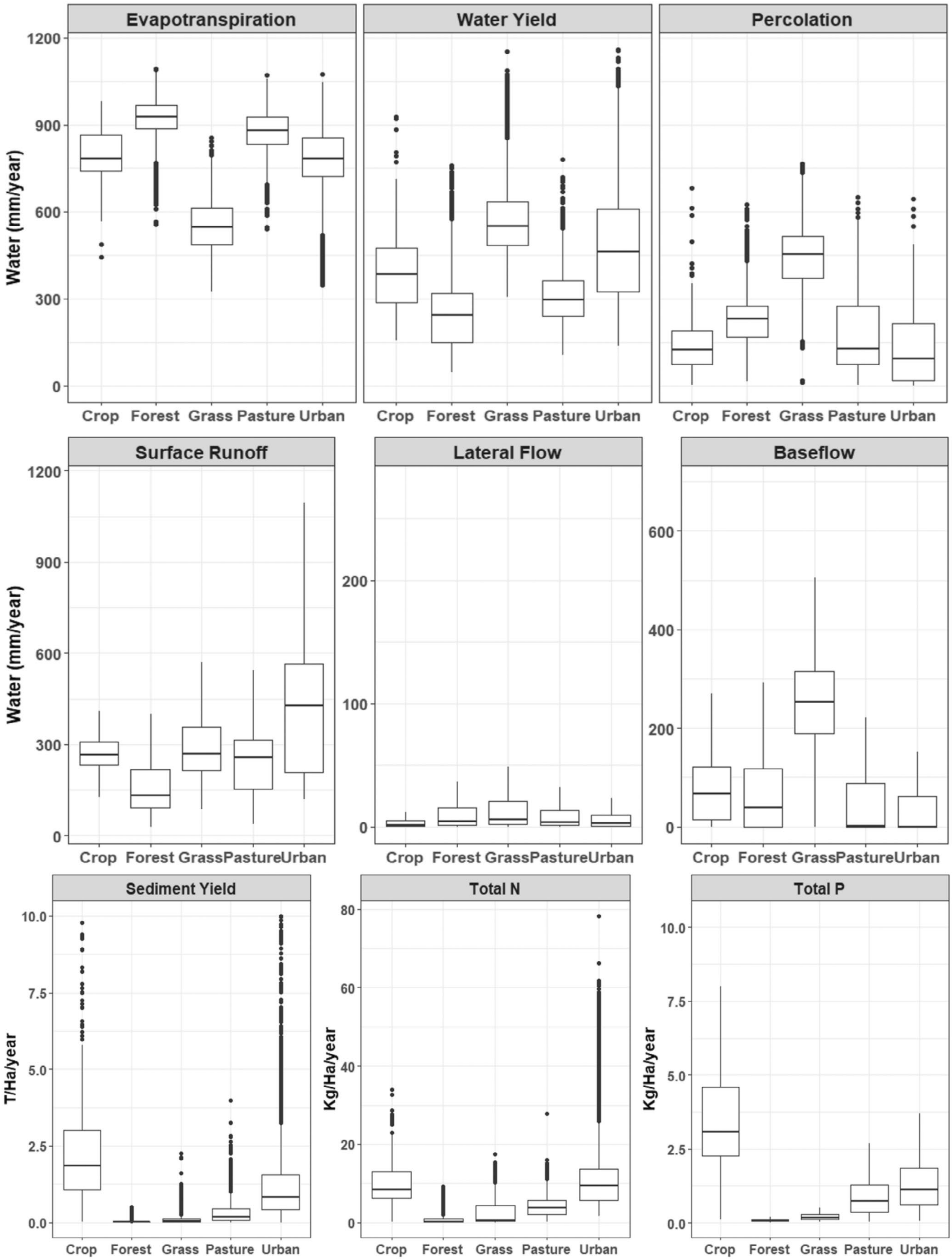

FIGURE 4 | Annual average water balance processes, runoff pathways (surface runoff, lateral flow, and groundwater flow), sediment (ton/ha/year), and nutrients (Total N and Total P) yield across different land use types.

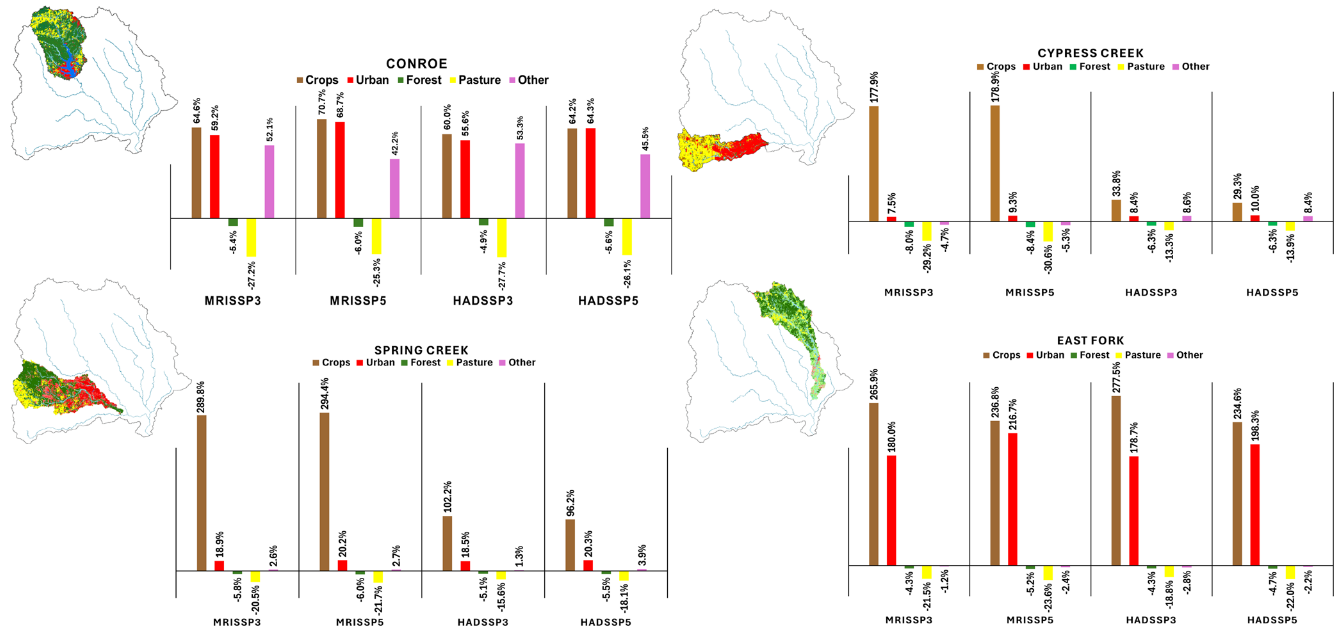

FIGURE 5 | Percentage change in land use from the baseline for tributary watersheds across the projected scenarios, with tributary watersheds considered up to the calibrated flow gauge sites. The baseline land use map and land classes for tributary watersheds are detailed in Figure 1.

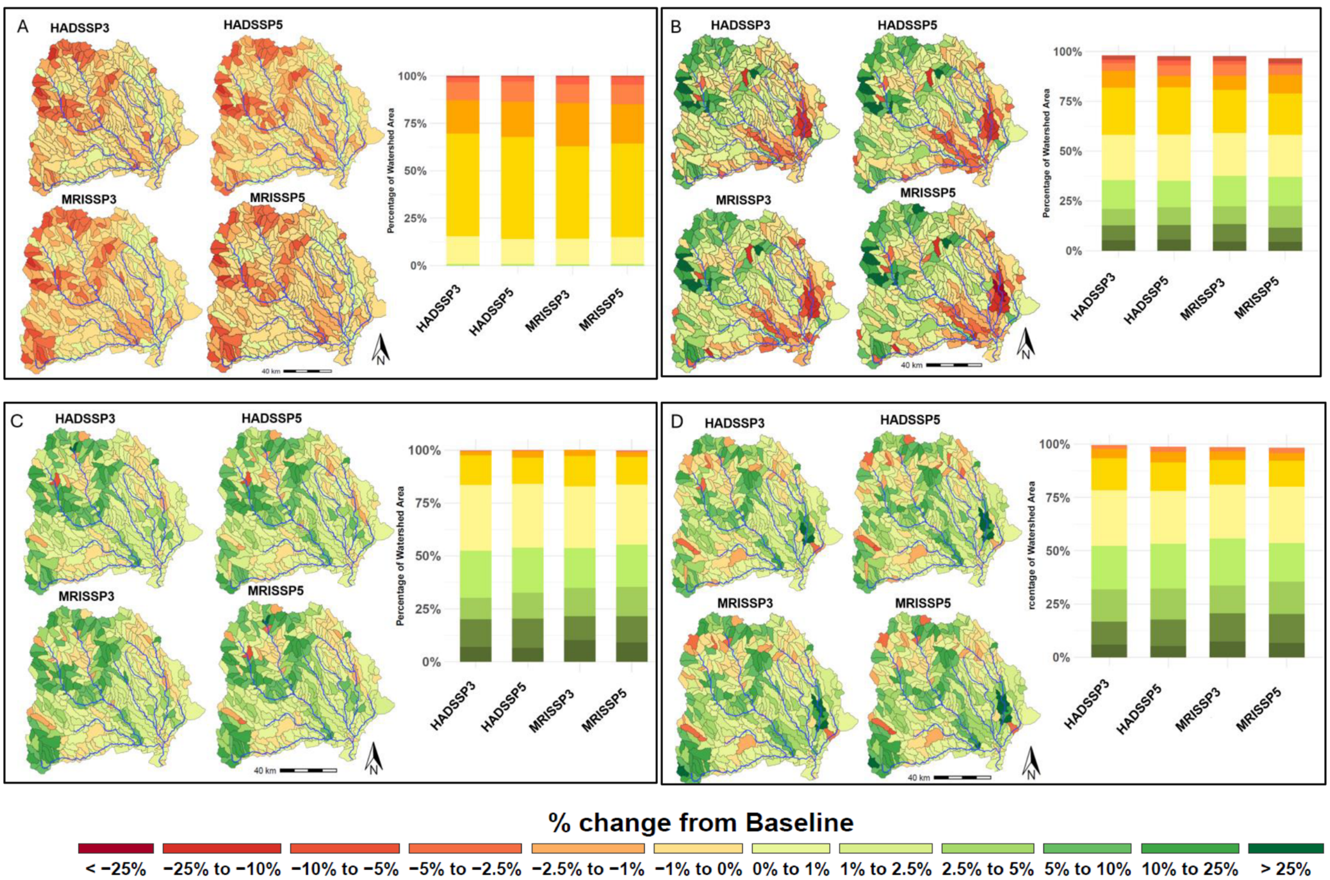

FIGURE 6 | Spatial distribution of percentage annual average difference from baseline for ET (A), percolation (B), water yield (C), and surface runoff (D) across sub-basins for all projected scenarios. Stacked bar charts show the percentage area of the watershed within defined ranges of differences from baseline.

Cypress Creek exhibited an approximately 4% increase under MRISSP3 and MRISSP5 and a 2% increase under HADSSP3 and HADSSP5 (Figure 7).

We developed daily flow duration curves (FDCs) for each selected reach to quantify the impact of land use change projections on flow characteristics. FDCs indicate the probability of

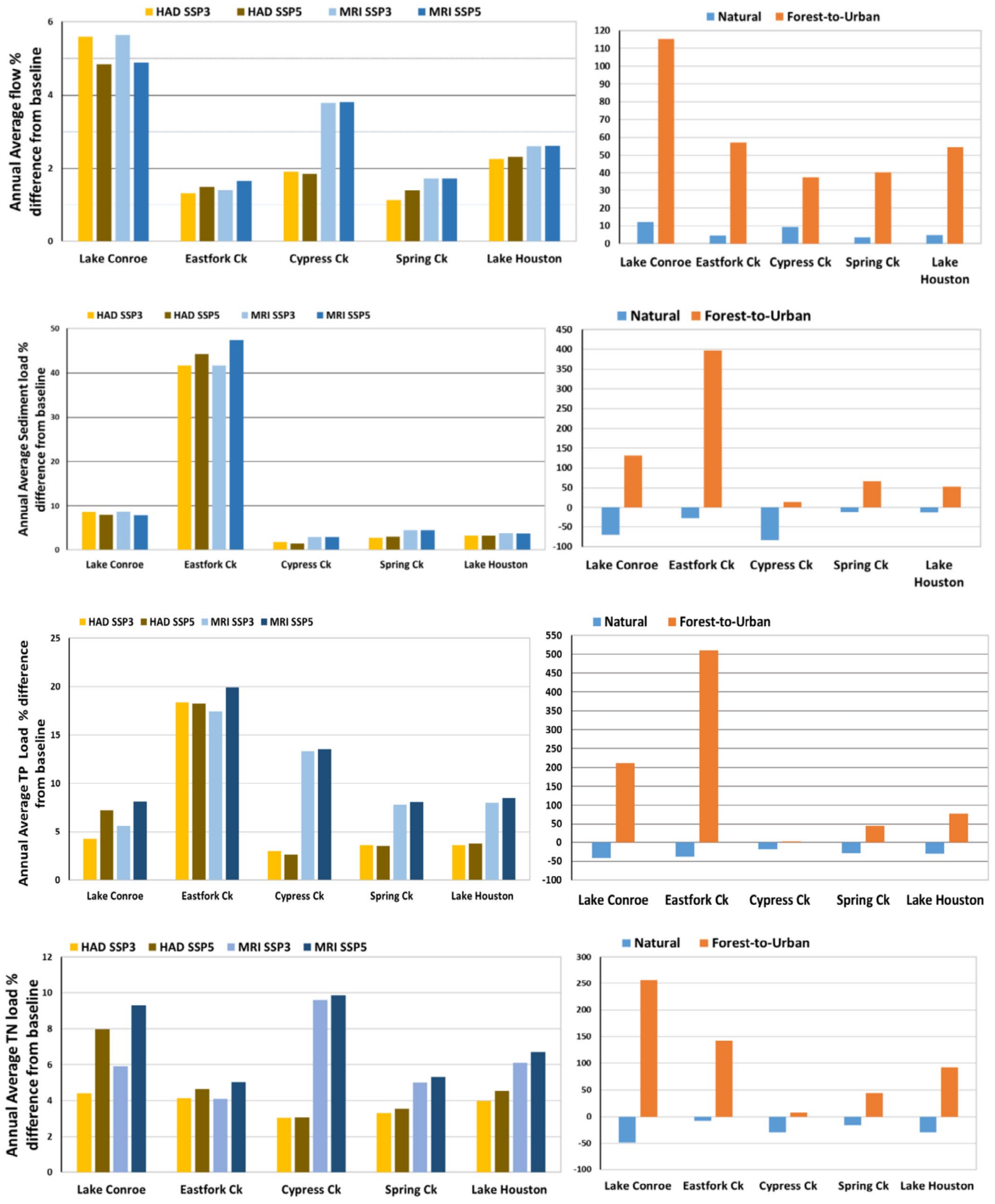

FIGURE 7 | Percent difference in annual average flow, sediment, TP, and TN loads with respect to baseline at selected streams flow calibration sites and at Lake Houston and Conroe for projected scenarios and extreme scenarios of "Natural" and "Forest-to-Urban".

a flow (Q) being equaled or exceeded (EPA 2007). We focused on the 90%, 50%, and 10% exceedance probabilities as these provide a reasonable bracket of low (90%), median (50%), and high (10%) flow characteristics (Vogel and Fennessey 1995). The FDC's revealed that maximum (Qmax) and high flows (Q10) were more impacted than low (Q90) and median (Q50) flows (Table S4, Figures 8 and 9). The MRISSP5 and MRISSP3 scenarios caused a relatively larger increase in Qmax and Q10 for

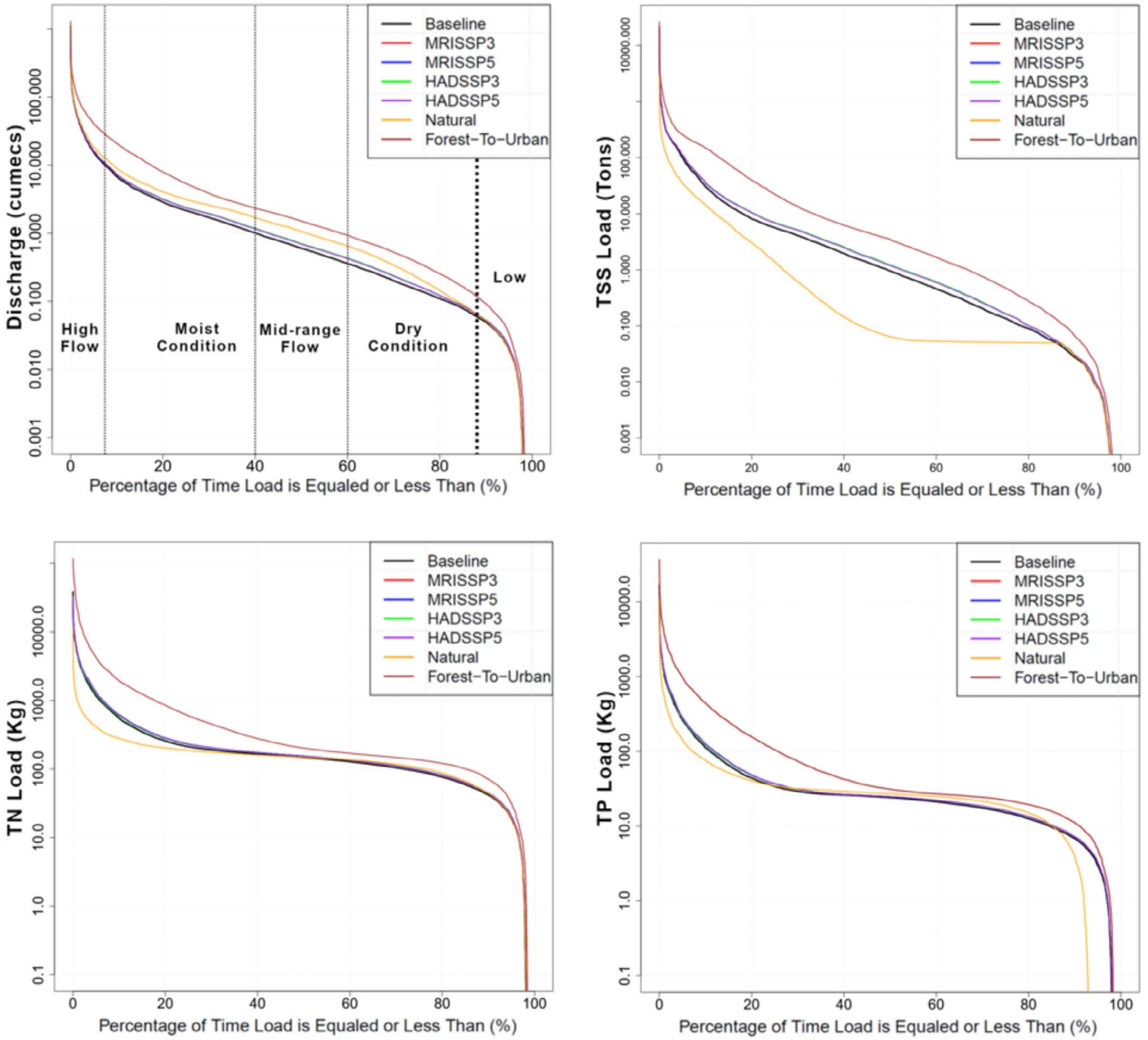

FIGURE 8 | Daily flow duration curve (FDC) and load duration curve (LDC) for TSS, TN, and TP at Lake Conroe across projected scenarios and extreme scenarios. The classification of flow at different exceedance probabilities is defined by EPA (2007).

all tributaries (Table S4). Qmax and Q10 for Lake Conroe were projected to increase by up to 7.3%. Similarly, peak flow in East Fork was projected to increase by 1.35%–1.83%, Spring Creek by 0.80%–1.2%, and Cypress Creek by 1.45%–2.82%.

The conversion of crops and pasture to grassland in the “Natural” scenario led to lower ET and higher water yield (Figure 4). This offset the streamflow reduction caused by converting urban areas to forests, which increased ET and reduced water yield. Annual average daily flow increased under the “Natural” scenario, with the largest impacts in Lake Conroe and Cypress Creek (approximately 10%) and smaller increases (approximately 5%) in other tributaries (Figure 7). In Lake Conroe, the conversion of 235.77 km^2 of pasture and 7.56 km^2 of cropland to grassland (Table S4) led to an approximately 30% increase in Q10 (6.83 to 9.83 m^3/s) and doubled Q50 (0.60 to 1.06 m^3/s), while Qmax and Q90 remained stable (Table S4, Figure 8). In Cypress Creek, converting 244.66 km^2 of urban areas to forest and 294.40 km^2 of pasture and 42.94 km^2 of cropland to grassland increased average flow by approximately 10%, nearly doubling Q50 (2.05 to 4.91 m^3/s) while leaving Qmax and Q10 unchanged. Similarly, in Spring Creek, Q50 rose by approximately 40% (2.62 to 3.68 m^3/s), though Qmax and Q10 were unaffected. Low flow (Q90) remained stable in both tributaries due to point source contributions. In the East Fork Creek sub-watershed, limited land-use changes consisting of 28 km^2 (2.83% of the sub-watershed) of urban area converted to forest and 95.20 km^2 (9.33% of the sub-watershed) of pasture to grassland caused minimal impact on the flow regime (Figure 9). In the “Forest-to-Urban” scenario, annual average flow increased across all tributaries and at the watershed outlet (Lake Houston), with the largest increase in Lake Conroe (> 100%), followed by East Fork Creek (60%) and Cypress and Spring Creeks (40%) (Figure 7). Q10 tripled in Lake Conroe (6.84 to 20.05 m^3/s) and increased by 60% in East Fork

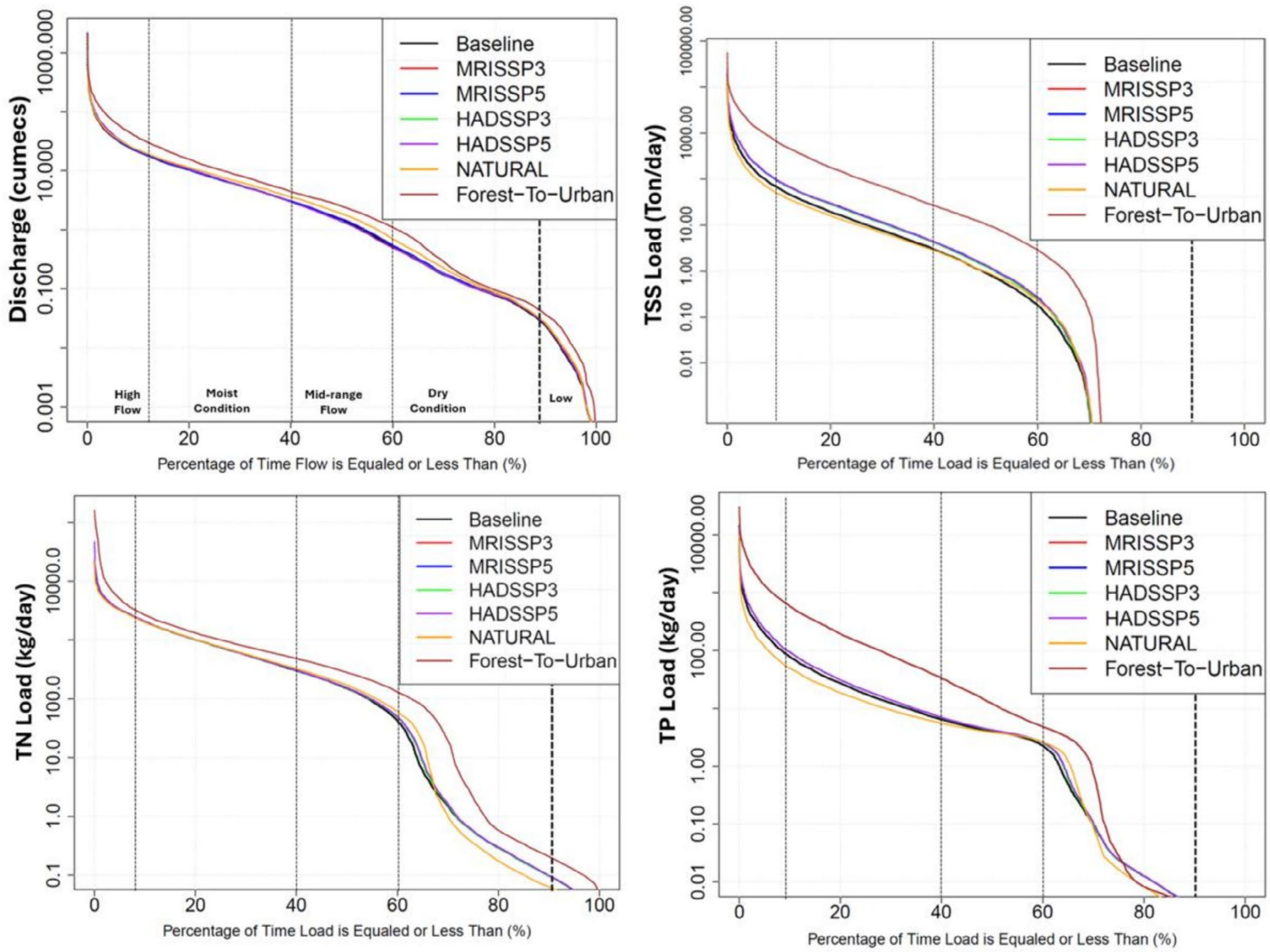

FIGURE 9 | Daily flow duration curve (FDC) and load duration curve (LDC) for TSS, TN, and TP for East Fork Creek across projected scenarios and extreme scenarios. The classification of flow at different exceedance probabilities is defined by EPA (2007). The TSS load after 70% exceedance probability is not shown since it is lower than 0.0001 tons/day.

Creek (22 to 36 m^3/s), 42% in Spring Creek (20.11 to 28.58 m^3/s), and 40% in Cypress Creek (16.2 to 22.65 m^3/s) while Q90 remained stable (Table S4). Overall, the annual average flow at the watershed outlet increased by 50%, with Q10 increasing by 64% and Q90 experiencing a twofold increase.

3.3.3 | Land Use Change Effects on Sediment

Approximately 67%–69% of the watershed was projected to have an increase in sediment yield under the future scenarios, while 30%–32% of the watershed was projected to experience a decrease (Figure 8). Larger percentage reductions in sediment yield (> 25%) were identified in a few sub-basins of Lake Conroe and Lake Creek, attributed to increases in grass/shrub land (Table S3); however, since baseline sediment yield in these areas was low, small absolute changes resulted in larger percentage reductions (Figure S6). Areas with over 100% increases in sediment yield (exceeding 1.25 tons/ha/yr from baseline) include upstream sub-basins of Cypress Creek for MRISSP3 and SSP5, due to a 177%–178% increase in cropland, the downstream region of East Fork Creek driven by a 178%–216% increase in urban areas, and the northwest corner upstream of Lake Conroe also influenced by urban expansion (Figure 5). These regions were also projected to have surface runoff increases (Figure 6) where upland soil erosion from runoff was a major contributing factor.

Similarly, annual average TSS loads for all selected reaches were projected to increase (Figure 7). The largest impact was on East Fork Creek showing a 40%–45% increase in load due to urban growth (> 150% from baseline, Figure 5), causing over a 100% increase in surface runoff (Figure 6) and subsequently flushing more sediment into the channels.

We also calculated load duration curves (LDC's), which, like FDCs, provide insight into the TSS, TN, and TP load exceedance probability (Johnson et al. 2009). We focused on the same exceedance probabilities (90%, 50%, 10%) as in the FDC analysis. Similar to streamflow responses to land use change, all reaches showed increases in TSS load for most exceedance probabilities across all projected scenarios (Table S4). High TSS loads (TSS10) increased by 37%–40% for East Fork (Figure 9, Table S4) and by 16%–19% for Conroe (Figure 8, Table S4), while minimal impacts were noted for Spring Creek (3%–4%), Cypress Creek (3%–5%), and Lake Houston (2%–3%). Low TSS loads (TSS90) were largely unaffected by land use projections.

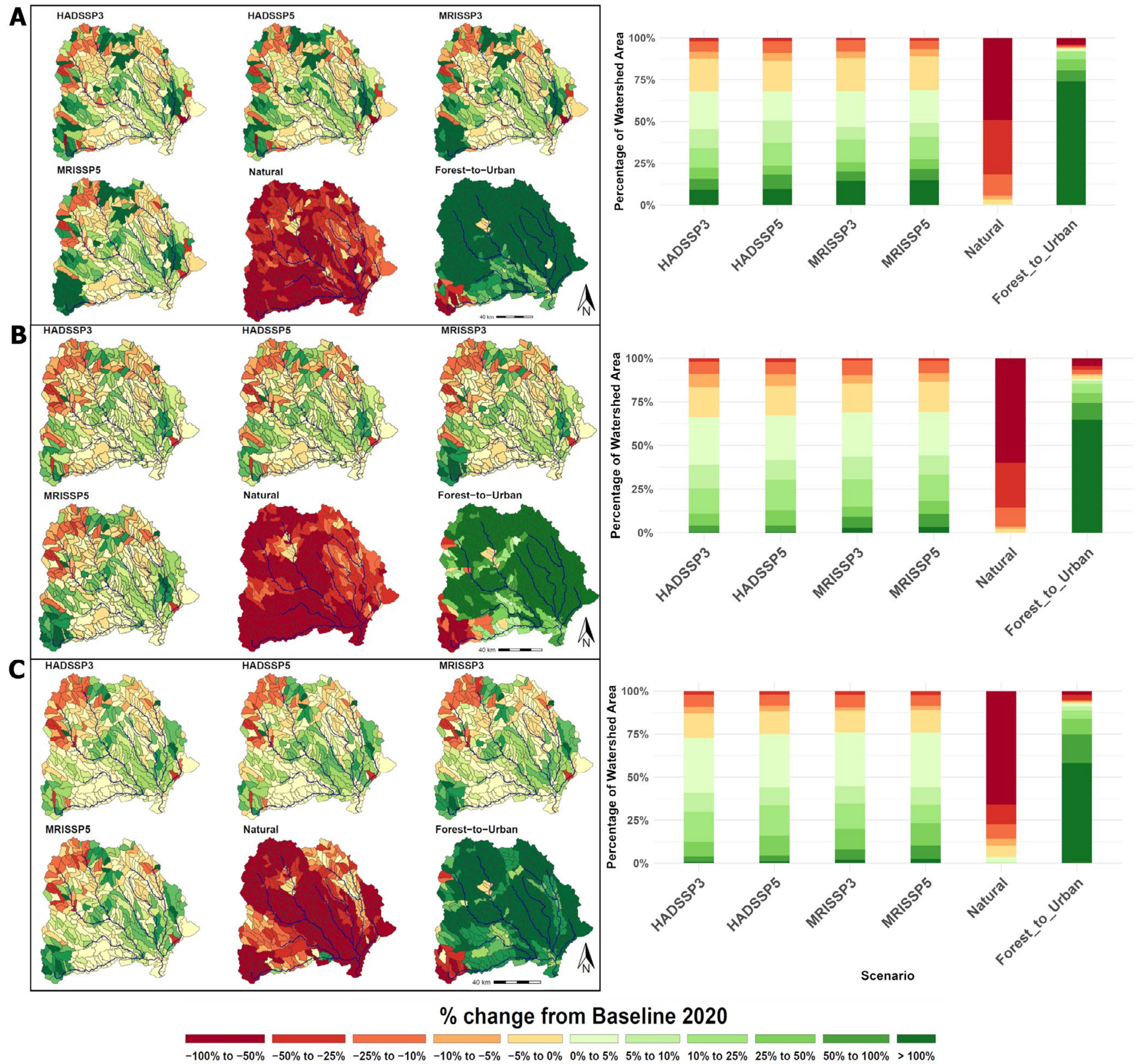

FIGURE 10 | Spatial distribution of TSS (A), TP (B), and TN (C) yield across the sub basins for all projected land use scenarios and extreme scenarios and percent of watershed area under defined ranges of load differences shown in bar chart.

Both extreme scenarios resulted in significant changes to sediment yield and TSS load compared to the baseline. In the "Natural" scenario, sediment yield decreased by 10% to over 50% across most of the watershed (Figure 10). In contrast, the "Forest-to-Urban" scenario resulted in sediment yield increases across most sub-basins, except in upstream Cypress Creek, where converting crop and pastureland to grassland reduced sediment yield by 25% to more than 50%. Annual average TSS loads under the "Natural" scenario decreased across all tributaries, ranging from 10% in Spring Creek and Lake Houston to 80% in Cypress Creek (Figure 7). High TSS loads (TSS10) decreased from 20% in Spring Creek to 95% in Cypress Creek (Table S4). Conversely, the "Forest-to-Urban" scenario led to TSS load increases from 15% in Cypress Creek to 400% in East Fork Creek. The impact of this scenario in urbanized Cypress Creek was minimal due to larger areas of pasture and cropland converted to grassland, which outweighed the smaller forest-to-urban conversions. The "Forest-to-Urban" scenario doubled both high (TSS10) and median (TSS50) TSS loads across all tributaries (Table S4).

3.3.4 | Land Use Change Effects on TP

Across future land use projections, 66%–69% of the watershed was projected to experience an increase in TP yield, while 31%–34% showed reductions (Figures 10 and S7). As expected, sub-basins with high TP yield corresponded to areas of high sediment yield. TP increases of over 50% (0.12–0.55 kg/ha/yr) (Figure S7) were projected in downstream sub-basins of East Fork Creek across all scenarios, while upstream sub-basins of Cypress Creek had projected TP yield increases exceeding 100% (0.24–1.91 kg/ha/yr) under MRISSP3 and SSP5 scenarios, driven by cropland expansion at the expense of pasture and forest land. Sub-basins of Lake Conroe with urban expansion increased TP yield by 10%–50%, whereas conversions to grassland or scrubland reduced TP yield by 5%–25%. Similar reductions in TP yield were projected for upstream Lake Creek sub-basins (0.03–0.15 kg/ha/yr).

Annual average TP load consistently increased at selected reaches across the projection scenarios (Figure 7). Urban expansion in downstream sub-basins in East Fork Creek resulted in larger increases in TP load (Figure 10). The pattern of annual average TP load changes was consistent with the pattern of TSS load. TP load at 10% exceedance probability (TP10) was projected to increase for all scenarios and all selected tributaries, ranging from increases of 3%–8% (Lake Houston) to 20%–22% (East Fork Creek), while median load (TP50) remained unaffected across four scenarios (Table S4, Figures 8 and 9).

Average annual TP yield decreased under the "Natural" scenario across most of the watershed (Figures 8 and S7). TP yield reductions under the "Natural" scenario were particularly evident in the Cypress Creek sub-watershed, where TP yield was reduced by 50–100% (0.70–1.26 kg/ha/yr). The annual average TP load at selected tributaries was projected to decrease under the "Natural" scenario from 10% (Cypress Creek) to nearly 50% (Lake Conroe) (Figure 7). Natural vegetation significantly reduced high loads (TP10) across tributaries with reductions ranging from 30% (East Fork) to 43% (Lake Houston). TP50 and TP90 (low load at 90% exceedance probability) remained largely unaffected for the "Natural" scenario in Spring and Cypress Creek due to point source contributions, while a 50% reduction in TP90 was estimated for Lake Conroe (Table S4). Contrastingly, the "Forest-to-Urban" scenario caused large variation in the annual average TP load increases, ranging from 1% (Cypress Creek) to 500% (East Fork Creek). The increase in TP load mostly impacted the high (TP10) load across all reaches except Cypress Creek, with the greatest impacts at East Fork Creek (increasing from 77.80 kg/day to 598.40 kg/day) and Lake Conroe (increasing from 112.10 kg/day to 441.90 kg/day). Annual average TP yield increased in the "Forest-to-Urban" scenario in almost all the northern upstream sub-basins by > 50% (1.05–1.81 kg/ha/yr) (Figure S7).

3.3.5 | Land Use Change Effects on TN

Projections of future land use indicated that 75% of the watershed could experience an increase in TN yield, with some areas exceeding a 100% increase (up to 4.32 kg/ha/yr from baseline) (Figures 10, S8). The largest increases in TN yield (50%–100%) were in the eastern sub-basins, driven by urban expansion and cropland conversion in East Fork, Peach, and Caney Creeks. In Lake Conroe's eastern region, TN yield was projected to increase by over 50% (0.55 to 4.32 kg/ha/yr), with similar increases in upstream sub-basins of Cypress Creek under MRISSP3 and SSP5. A 10%–25% reduction in TN yield (0.20 to 1.55 kg/ha/yr) was projected in the northwest portion of the watershed, including Lake Creek and Lake Conroe sub-watersheds. Annual average TN loads were projected to increase across all selected tributaries and scenarios, with MRISSP5 showing the highest increases, ranging from 5% (East Fork Creek) to 10% (Cypress Creek) (Figure 7). The daily TN load distribution (Figures 8 and 9, Table S4) showed that East Fork Creek was the least impacted, as urban expansion in the downstream sub-basins was compensated for by the less impacted upstream region due to its unchanged forested and natural land uses (Figure 10). High TN load (TN10) was estimated to be relatively more impacted than median (TN50) and low (TN90) load for all tributaries and scenarios. Projected increases in TN10 ranged from ~0.3% (East Fork Creek) to 7%–12% (Lake Conroe). In contrast, TN50 showed smaller increases ranging from 0.01%–0.3%.

(East Fork Creek) to ~5% (Lake Conroe) while TN90 increased < 1% for all tributaries except Lake Conroe (5%–6%).

In the "Natural" scenario, TN yield decreased across all sub-basins, with reductions ranging from 0.50 to 9.75 kg/ha/yr, representing up to ~100% reductions. Annual average loads reduced largely in Lake Conroe (~50%), while East Fork Creek exhibited the smallest reduction (~5%) (Figure 7). The greatest reductions were observed in high TN loads (TN10), with decreases ranging from 10% in East Fork Creek to 50% in Lake Conroe. Conversely, the "Forest-to-Urban" scenario led to an increase in TN yield across all sub-basins, particularly affecting downstream areas of Peach and Caney Creek and in the vicinity of Lake Conroe, where yield increased by over 100%. Notably, upstream Cypress Creek showed a 25 to more than 50% reduction in TN yield due to pasture and cropland conversion to grassland under the "Forest-to-Urban" scenario. Except for the urbanized Cypress Creek, converting forests to urban areas increased high TN loads (TN10), with increases ranging from 14% (Spring Creek) to 250% (Lake Conroe).

4 | Discussion

We evaluated the effects of land use changes on hydrological processes and water quality in the San Jacinto watershed, Texas, using SWAT. The calibrated baseline model was applied to four projected land cover scenarios for 2070 and two hypothetical scenarios reflecting "Forest-to-Urban" and "Natural" land cover. Results indicated that streamflow, TSS, TN, and TP loads generally increased across major tributaries in the watershed under future projections, though the magnitude of change varied across the watershed, influenced by local hydroclimatic conditions, soil type, and specific land use changes. For instance, in the East Fork Creek sub-watershed, conversion from forested land to developed areas led to a 1.5% rise in annual average streamflow, a 40% increase in TSS load, a 20% increase in TP load, and a 5% increase in TN load. Our analysis revealed that land use change significantly impacted daily high flows, TSS, and nutrient loads more so than median or low flows or loads, highlighting a critical aspect of hydrological responses to urbanization. This spatially explicit analysis identified regions of the watershed sensitive to deforestation, urban expansion, and crop expansion, in terms of water yield, surface runoff alteration, soil erosion, and their subsequent effects on stream water quality. The findings thus underscore critical considerations for land and water management in this developing watershed, particularly the need to address the interactions between climate variability, urban expansion, and increasing water demand. Management strategies would be most effective if they consider local hydroclimatic conditions, soil types, and the specific impacts of various land use changes on hydrological processes and water quality.

4.1 | Land Use Linkages to Water Quantity and Quality

Our modeled water balance, flow generation processes, and sediment and nutrient yields align with previous studies in the San Jacinto watershed (Table 4) and vary significantly across land use types. Consistent with previous studies (Sun et al. 2011; Caldwell et al. 2012; Li et al. 2020), forested sub-basins had lower water yield due to higher ET rates while exhibiting higher percolation and lower surface runoff, benefiting groundwater recharge and sustaining baseflow (Texas Natural Resource Conservation Commission 1999) contribution to the stream. The spatial patterns and ranges of our simulated annual average ET (Figure 3) were comparable with those reported by Reitz et al. (2017) (Figure S9), which integrated remote sensing and water-balance methods to generate an ET dataset for the conterminous U.S. Specifically, ET was lower in urban-dominated areas such as Cypress Creek and Spring Creek, reflecting limited vegetation and extensive impervious cover, and higher in forested areas, indicating that the model captures land use–dependent variations in ET. The SWAT-simulated ET/precipitation (ET/PCP) ratio for our watershed (0.65) aligns closely with the range reported by Reitz, Sanford, et al. (2017); Reitz, Senay, and Sanford (2017) for southeast Texas (0.61–0.80), providing further confidence in the model's representation of water balance. Similarly, the simulated surface runoff-to-precipitation ratio (0.16) falls within the range reported for small to large watersheds in the Texas Blackland Prairie Ecoregion (0.12–0.17) (Harmel, Richardson, et al. 2006; Harmel, Potter, et al. 2006). Simulated surface runoff across land uses is also comparable with past studies (Table 4), with the highest values from urban areas (150–1000 mm/yr), followed by cropland (150–400 mm/yr), pasture (50–500 mm/yr), grassland (100–500 mm/yr), and forest (50–400 mm/yr). While surface runoff dominates in urban and cropped areas, a crucial counter-process in grassland is the generation of baseflow. Grassland, with its deep root systems, facilitates greater infiltration, thus contributing more baseflow than surface runoff (Wilcox et al. 2007). Long-term analysis in the semi-arid rangelands of Central Texas has shown that baseflow has remained essentially consistent or has increased slightly over decades, even as stormflows have decreased, suggesting that changes in rangeland condition have favored infiltration over runoff (Wilcox et al. 2008). Studies of Texas rangelands by the Texas Water Development Board (TWDB) (Knight et al. 1995; Wilcox 2002; Wilcox et al. 2003) demonstrated improved subsurface flow using various grass and shrub species, with outcomes varying by soil type, depth, slope, and rainfall. These findings align with our results, which indicate that grasslands can enhance baseflow.

In contrast, urban land use showed the highest water yield and surface runoff, with the lowest percolation rates. Our study found urbanization and agricultural expansion led to a 5% to 25% ET reduction and more than a 10% increase in surface runoff (Figure 6A,D). Similar trends were observed in other investigations of southern U.S. watersheds; Khan (2005) reported that an 88% increase in impervious surfaces in Houston increased the runoff ratio by over 15%, and Dow and DeWalle (2000) found significant ET reductions in 51 eastern and southern U.S. watersheds due to urbanization and residential development.

Similarly, sediment and nutrient yields were highly dependent on land use and land management practices. Sediment, TN, and TP yields from forests and grassland were clearly lower than those of other land uses, with cropland producing the highest yields, followed by urban land use. Caldwell et al. (2023) found similar relationships between land use and sediment and nutrient loading based on examination of monitoring data, showing that a 1% change from forest to developed land cover could result in an approximately 1.5% increase in TN concentration, a 1.9% increase in TP concentration, and a 0.4% increase in TSS concentration, while a 1% change from forest to agriculture resulted in even higher percent changes in sediment and nutrient concentration. Land use changes due to agriculture and urbanization can increase the sediment yield due to an increase in soil erosion and wash load from impervious surfaces (Kidane et al. 2019; Gashaw et al. 2019; Tumsa et al. 2023). Urbanization and deforestation, which increase impervious surfaces and barren land, increase surface runoff, leading to higher streamflow and greater sediment loads from stream channel erosion (Allmendinger et al. 2007; O'Driscoll et al. 2010). TN and TP yields can increase with urbanization and conversion to agriculture through practices such as fertilizer and manure application (Rebich et al. 2011). Our results align with the literature, as seen in Cypress Creek where upstream sub-basins were projected to experience more than a 25% increase in TP and TN yield due to the conversion of pasture and grassland into croplands. The "Natural" and "Forest-to-Urban" land use scenarios demonstrate the ability of natural landscapes to regulate high flows and water quality, as well as the risks posed by land conversion to development that undermines these vital ecosystem services.

The Soil and Water Assessment Tool (SWAT) model successfully simulated hydrologic and sediment transport processes in the watershed, with the surface runoff-to-precipitation ratio (0.16) aligning well with the regional range of 0.12–0.17 reported by Harmel, Richardson, et al. (2006); Harmel, Potter, et al. (2006) for the Texas Blackland Prairie. Furthermore, the SWAT simulations of runoff and sediment yield were consistent across various land uses: for croplands, the model's runoff (150–450 mm/yr), sediment (up to 5 tons/ha/year), TN (up to 30 kg/ha/yr), and TP (up to 7.5 kg/ha/yr) closely matched long-term field data from the MANAGE database (Harmel, Richardson, et al. 2006; Harmel, Potter, et al. 2006; Harmel et al. 2008) and White et al. (2015) (Table 4), and also compared well with field data from cornfields in the Texas Blackland Prairie (110–330 mm runoff, sediment up to 4.5 tons/ha/yr, TN up to 27 kg/ha/yr, TP 3.5–7.0 kg/ha/yr). While grasslands generated negligible sediment, runoff generated up to 400 mm/yr; the overall pattern of land use-dependent sediment yield (cropland > urban > natural vegetation) mirrored results for the conterminous US reported by Woznicki et al. (2020).

4.2 | Projected Land Use Change and Effects on Water Resources

Land use projections for the San Jacinto watershed indicate a continued shift of pasture, grassland, and forest, with increased

TABLE 4 | Summary of comparisons of water balance, sediment, and nutrient yield to other studies in the literature.

Hydrologic component	Variable	Land use	This study (range or value)	Literature range	Literature reference(s)
A. Water Balance	(ET, mm/yr)	Watershed	600–1500	600–1500	(Reitz, Sanford, et al. 2017; Reitz, Senay, and Sanford 2017)
	ET/Precipitation		0.65	0.61–0.80	(Reitz, Sanford, et al. 2017; Reitz, Senay, and Sanford 2017)
	Surface Runoff/ Precipitation		0.16	0.12–0.17	(Harmel, Richardson, et al. 2006; Harmel, Potter, et al. 2006)
	ET (mm/yr)	Forest	600–1000	500–1100	(Scanlon et al. 2005)
		Grassland	300–800	500–900	(Scanlon et al. 2005)
	Surface Runoff (mm/yr)	Urban	150–1000	550–1100	(Rose and Peters 2001; Sui and van de Ven 2023; Williams 2025)
		Cropland	150–400	0–500	(White et al. 2015)
		Grassland	100–500	0–400	(White et al. 2015)
B. Sediment Yield	Sediment Yield (tons/ha/yr)	Cropland	0–7	0–10	(White et al. 2015)
				0–20	(Harmel, Richardson, et al. 2006; Harmel, Potter, et al. 2006; Harmel et al. 2008)
				> 5	(Woznicki et al. 2020)
		Grassland/ Forest	0 – 1	0–1	(White et al. 2015)
				0–5	(Harmel, Richardson, et al. 2006; Harmel, Potter, et al. 2006; Harmel et al. 2008)
				Negligible	(Woznicki et al. 2020)
		Urban	0–3	0–3	(Woznicki et al. 2020)
C. Nutrient Yield	Total Nitrogen (TN kg/ha/yr)	Cropland	0–20	0–50	(White et al. 2015; Harmel, Richardson, et al. 2006; Harmel, Potter, et al. 2006; Harmel et al. 2008; Beaulac and Reckhow 1982)
		Grassland	0–10	0–10	(White et al. 2015; Harmel, Richardson, et al. 2006; Harmel, Potter, et al. 2006; Harmel et al. 2008)
		Urban	0–25	5–50	(White et al. 2015; Beaulac and Reckhow 1982)
	Total Phosphorus (TP kg/ha/year)	Cropland	0–7.5	0–5	(White et al. 2015)
		Grassland/ Forest	< 1	0–1	(White et al. 2015; Harmel, Richardson, et al. 2006; Harmel, Potter, et al. 2006; Harmel et al. 2008; Beaulac and Reckhow 1982)
		Urban	0–4	0–6	(White et al. 2015; Beaulac and Reckhow 1982)

urbanization and cropland by 2070. Urban land use is expected to rise from 15% of the watershed in 2020 to 20% in 2070, while forest land may decrease from 55% to 51%. Although cropland comprised only 1% of the watershed in 2020, it was projected to more than double in some scenarios by 2070. The impact of land use change on water yield and water quality was projected to be relatively minor at the watershed scale but was larger at smaller scales within the watershed due to the spatial variability of projected land use change. For example, the northeastern region upstream of Lake Conroe and the southeastern East Fork sub-watershed were projected to experience substantial urban expansion (+68% and +216%, respectively), leading to notable changes in water quality (Figure 5, Table S3).

While total water yield was projected to have little change under the land use projections, our results show that the sources of water yield could potentially change, with implications for water quality. For instance, a modest 2.5%–10% increase in water yield was observed in the East Fork, while sediment yield increased by 25%–100%, largely driven by a $>25\%$ increase in surface runoff associated with expanding impervious surfaces. Similar findings have been reported in southeastern U.S. watersheds, where a 10%–40% increase in impervious surfaces significantly impacts runoff and streamflow (Brun and Band 2000; Paul and Meyer 2001; Boggs and Sun 2011; Sun et al. 2015). Our study estimated that increased surface runoff from urbanization resulted in a 10% increase in TSS load to Lake Conroe and 40% in East Fork Creek. Although urban expansion had a minimal effect on East Fork's annual average streamflow (2%), it increased TSS and TP loads by 40% and 20%, respectively. In the southwestern region, the Cypress Creek area experienced over a 25% more runoff, leading to a 2% rise in peak flow, a maximum ~15% increase in TP load, and ~10% increase in TN load, due to a $76\,\text{km}^2$ cropland expansion. These localized increases in TSS and nutrient loads driven by diffuse pollution from expanded impervious surfaces and cropland could complicate water quality regulation compared to point source pollution. Hence, our results show the importance of considering land use change at a finer scale while assessing the impacts of land use alterations within the larger watershed.

4.3 | Implications for Water Management

Our work showed that urbanization and agricultural expansion can cause long-term hydrological shifts by reducing ET and increasing surface runoff, sediment, and nutrient loads. Urbanization and associated increased impervious surfaces raise flood risks (Wheater and Evans 2009) and sediment loads (Nguyen et al. 2022). While projected increases in maximum (Qmax) and high (Q10) flows were small under the future land use scenarios, the "Natural" and "Forest-to-Urban" scenarios demonstrate the overall potential impact of urbanization on high flows and sediment and nutrient loads. For example, Lake Conroe was projected to experience a 13% increase in Qmax and a 134% increase in Q10 under the "Forest-to-Urban" scenario, while Q50 was projected to increase 100%. In contrast, maintaining natural vegetation, such as forests and grassland, supports water sustainability, resulting in a 10% increase in water yield while keeping Qmax and Q90 stable with moderate increases in Q50.

Urban diffuse/non-point source pollution and agricultural land management practices increase sediment and nutrient loads, exacerbating reservoir sedimentation and contributing to eutrophication (Russell et al. 2017). Many recent studies have emphasized the importance of natural grassland as an effective nature-based solution in reducing sediment yield (Robotham et al. 2023). Our study supported that while natural vegetation has a modest impact on the water budget, its ability to reduce TSS load is substantial. For example, deforestation and urbanization in East Fork Creek were projected to increase TSS load by 45% under future scenarios and ~400% under the "Forest-to-Urban" scenario, whereas natural landscapes reduced TSS load by 20%. For Lake Conroe, TSS load decreased by 50%, with an 85% reduction in load during peak flows (21,200 tons/day to 2826 tons/day) under the "Natural" scenario (Table S4). Reducing TSS load also contributes to decreases in TP loads by 50%, helping prevent eutrophication in Lake Conroe. Natural vegetation, including grassland and forest land uses, could balance water availability with sediment and nutrient load reduction in urban-dominated watersheds such as Cypress Creek. This suggests that a balanced approach to land use alterations, preserving sufficient forest and other natural areas while planning for urban expansion, could stabilize hydrological processes and minimize sediment and nutrient load.

4.4 | Limitations and Opportunities for Future Research

The results of this study should be interpreted while considering the limitations and uncertainties associated with future land use projections and hydrological modeling in general. Uncertainties in model inputs, structure, parameters, and future land use estimates can compound, affecting the accuracy of hydrology and water quality predictions (Suttles et al. 2018). Limitations of hydrological models are related to uncertainty in input data and uncertainty in how hydrologic and water quality processes are simplified and represented (Caldwell et al. 2023). Limited availability and uncertainties in monitoring data can impact the representation of hydrological and water quality processes because model parameters are calibrated within well-constrained boundaries using measured flow, sediment, and nutrient data. For instance, in our watershed, the lack of sufficient TN monitoring sites reduced the spatial accuracy of nutrient parameter representation. Additionally, possible measurement errors in sediment and nutrient concentrations further contribute to the overall uncertainty in model calibration and evaluation. Lastly, the monthly observed sediment and nutrient load, estimated using LOADEST (a regression-based model) from discrete concentration and streamflow data, is subject to inherent uncertainty.

Uncertainty in land use projections can also translate into uncertainty in hydrologic model results. The intent of the land use projections developed as part of the Forest Service Resources Planning Act Assessment was not to provide predictions of potential future conditions; rather, the intent was to provide a range of plausible conditions that can be used to assess how systems may respond to different rates of change or how different decisions may alter resource trajectories (Langner et al. 2020; Moss et al. 2008). Projected land use changes over space and time carry uncertainty and should not be viewed in a probability context nor as a prediction with a certain level of accuracy

(Caldwell et al. 2024). This spatial uncertainty can increase with increasing spatial resolution (Brooks et al. 2020), for example, when downscaling from the county to a fine-scale grid.

Our results underscore the need to evaluate local land use impacts on streamflow and water quality in large-scale watershed assessments. Hydrological models such as SWAT, combined with future land use scenarios under a range of future scenarios, can help identify areas most at risk from continued development, aiding watershed planners and informing policy decisions. This approach applies to similar watersheds in the Southeast USA and other regions experiencing rapid urban sprawl, which displaces forests and natural vegetation and degrades water quality. Our results provide site-specific potential water quality and quantity concerns in the San Jacinto, a critical developing watershed, showing that land use change could directly impact Lake Conroe and Lake Houston, which serve as the principal reservoir for the city of Houston. Thus, our model can help inform future decision-making or model development for targeted water resource evaluations. For example, future research efforts could use this modeling framework to improve risk assessments of severe flooding events (e.g., Hurricane Harvey in 2017 with a return period over 100 years) in vulnerable and previously impacted areas such as the Houston metropolitan region.

This study provides a detailed, spatially explicit examination of the potential effects of land use change in a critical developing water supply watershed that could be a foundation for future research. For example, integrating climate change projections could refine predictions for high-return-period flood peaks and impact reservoir management. Given our land use projections results, Lake Conroe could experience a 6% increase in annual average streamflow and a 10% increase in sediment load, reducing reservoir storage capacity over time due to sediment accumulation. While this study offers reliable estimates of sediment yield across various land uses, integrating a hydrodynamic model in future research could further enhance predictions of sediment deposition rates at different reservoir levels.

Additionally, the impact of changing point source loads, such as wastewater treatment plants, attributed to urban expansion was not considered; their inclusion could further increase nutrient loads and jeopardize reservoir water quality through eutrophication. The simulated "Natural" scenario in our study confirmed that prioritizing forest and grassland conservation within a watershed could help buffer recurrent flooding and sustain water yield. Therefore, conserving forest and grassland areas could be a tool for watershed planners in mitigating the effects of population growth and associated land use change (Gagrani et al. 2014; Olander and Young 2016). As urban development and population growth continue, further research is needed to find a balanced approach to land use changes that preserves sufficient forest and natural areas, stabilizes hydrological processes, and prevents extreme variations in water yield and other components.

5 | Conclusions

This study quantified the effects of projected future land use changes on water quantity and quality in major tributaries and water supply reservoirs at a fine scale, and identified sensitive areas that exhibit strong water quality responses to land use change in the forest-dominated but urbanizing San Jacinto watershed. We found that sediment and nutrient loads could increase substantially by 2070 in some tributaries and reservoirs; however, these findings were highly location- and scale-specific, emphasizing the importance of focusing on sensitive local areas for watershed management and land use planning. Hydrologic response to land cover alteration is highly variable at a fine scale and is influenced by multiple factors such as climate, soils, vegetation characteristics, and land management practices. By integrating detailed, fine-scale land use projections in a hydrologic modeling framework, vulnerable regions within a watershed can be identified, helping to predict changes in both water quantity and water quality. This framework can provide critical information for resource managers, aiding in the development of strategies to adapt to or mitigate the adverse effects of urbanization, deforestation, and agricultural expansion on water quality and flood risks in diverse environmental contexts worldwide.

Author Contributions

Sagarika Rath: conceptualization, methodology, data curation, writing – review and editing, writing – original draft, formal analysis. **Peter Caldwell:** writing, review and editing, methodology, investigation. **Sam Moore:** formal analysis, visualization, data curation. **Patricia Spellman:** writing, review and editing. **Raghavan Srinivasan:** funding acquisition, project administration. **Jeff Arnold:** review and editing. **Katie Martin:** review and editing. **Ge Sun:** review and editing. **Georgianne Moore:** review and editing. **James Vose:** review and editing.

Acknowledgments

We gratefully acknowledge the feedback of the Associate Editor and reviewers whose insightful comments led to an improved manuscript. This study was supported by the U.S. Department of Agriculture (USDA) Forest Service, Southern Research Station by agreement number 20JV-11330180-016 to Dr. Raghavan Srinivasan at Texas A&M University. Any opinions, findings, conclusions, or recommendations expressed in the material are those of the authors and do not necessarily reflect the views of the USDA or Texas A&M University. Any use of trade, firm, or product names is for descriptive purposes only and does not imply endorsement by the U.S. Government.

Funding

This work was supported by the U.S. Department of Agriculture.

Conflicts of Interest

The authors declare no conflicts of interest.

Data Availability Statement

The data that support the findings of this study are available from the corresponding author upon reasonable request.

References

2023. "Water Resource Mission Area, USGS." https://www.usgs.gov/mission-areas/water-resources.

7, B. P., Y. U. N. Huang, and J. W. Walker. 2008. "Long-Term Trends in Streamflow From Semiarid Rangelands: Uncovering Drivers of Change." *Global Change Biology* 14, no. 7: 1676–1678.

Abbaspour, K. C. 2012. *SWAT-CUP 2012. SWAT Calibration and Uncertainty Program: A User Manual*. Swiss Federal Institute of Aquatic Science and Technology.

Abbaspour, K. C. 2015. "SWAT Calibration and Uncertainty Programs. A User Manual." 103, 17–66.

Allmendinger, N. E., J. E. Pizzuto, G. E. Moglen, and M. Lewicki. 2007. "A Sediment Budget for an Urbanizing Watershed, 1951-1996, Montgomery County, Maryland, USA 1." *JAWRA Journal of the American Water Resources Association* 43, no. 6: 1483–1498.

Arnold, J. G., D. Moriasi, P. Gassman, et al. 2012. "SWAT: Model Use, Calibration, and Validation." *Transactions of the ASABE* 55: 1491–1508.

Arnold, J. G., and R. Srinivasan. 1998. "Large Area Hydrologic Modeling and Assessment. I: Model Development." *Journal of the American Water Resources Association* 34, no. 1: 73–89.

Beaulac, M. N., and K. H. Reckhow. 1982. "An Examination of Land Use-Nutrient Export Relationships 1." *JAWRA Journal of the American Water Resources Association* 18, no. 6: 1013–1024.

Benaman, J., and C. A. Shoemaker. 2005. "An Analysis of High-Flow Sediment Event Data for Evaluating Model Performance." *Hydrological Processes* 19: 605–620. https://doi.org/10.1002/hyp.5608.

Bieger, K., G. Hörmann, and N. Fohrer. 2015. "The Impact of Land Use Change in the Xiangxi Catchment (China) on Water Balance and Sediment Transport." *Regional Environmental Change* 15: 485–498.

Boggs, J. L., and G. Sun. 2011. "Urbanization Alters Watershed Hydrology in the Piedmont of North Carolina." *Ecohydrology* 4, no. 2: 256–264.

Brath, A., A. Montanari, and G. Moretti. 2006. "Assessing the Effect on Flood Frequency of Land Use Change via Hydrological Simulation (With Uncertainty)." *Journal of Hydrology* 324, no. 1–4: 141–153.

Brody, S. D., J. Gunn, W. Peacock, and W. E. Highfield. 2011. "Examining the Influence of Development Patterns on Flood Damages Along the Gulf of Mexico." *Journal of Planning Education and Research* 31, no. 4: 438–448.

Brooks, E. B., J. W. Coulston, and K. H. Riitters. 2020. "Using a Hybrid Demand-Allocation Algorithm to Enable Distributional Analysis of Land Use Change Patterns." *PLoS One* 15, no. 10: e0240097. https://doi.org/10.1371/journal.pone.0240097.

Brooks, E. B., J. W. Coulston, K. H. Riitters, and D. N. Wear. 2023. "Spatial Realizations of County-Level Land Use Projections for the Conterminous United States, 2020–2070, Used in the 2020 RPA Assessment."

Brun, S. E., and L. E. Band. 2000. "Simulating Runoff Behavior in an Urbanizing Watershed." *Computers, Environment and Urban Systems* 24, no. 1: 5–22.

Caldwell, P. V., K. L. Martin, J. M. Vose, et al. 2023. "Forested Watersheds Provide the Highest Water Quality Among All Land Cover Types, but the Benefit of This Ecosystem Service Depends on Landscape Context." *Science of the Total Environment* 882: 163550.

Caldwell, P. V., G. Sun, S. G. McNulty, E. C. Cohen, and J. A. Moore Myers. 2012. "Impacts of Impervious Cover, Water Withdrawals, and Climate Change on River Flows in the Conterminous US." *Hydrology and Earth System Sciences* 16: 2839–2857.

Caldwell, P. V., J. M. Vose, J. K. Costanza, et al. 2024. "Water: An Analysis to Support the Southern Forest Outlook." Gen. Tech. Rep. SRS-276. Asheville, NC: U.S. Department of Agriculture, Forest Service, Southern Research Station. 60 p. https://doi.org/10.2737/SRS-GTR-276.

Callender, E., and K. C. Rice. 2000. "The Urban Environmental Gradient: Anthropogenic Influences on the Spatial and Temporal Distributions of Lead and Zinc in Sediments." *Environmental Science & Technology* 34, no. 2: 232–238.

Chen, M., P. W. Gassman, R. Srinivasan, Y. Cui, and R. Arritt. 2020. "Analysis of Alternative Climate Datasets and Evapotranspiration Methods for the Upper Mississippi River Basin Using SWAT Within HAWQS." *Science of the Total Environment* 720: 137562.

Chilagane, N. A., J. J. Kashaigili, E. Mutayoba, et al. 2021. "Impact of Land Use and Land Cover Changes on Surface Runoff and Sediment Yield in the Little Ruaha River Catchment." *Open Journal of Modern Hydrology* 11, no. 3: 54–74.

Conlon, K., A. Monaghan, M. Hayden, and O. Wilhelmi. 2016. "Potential Impacts of Future Warming and Land Use Changes on Intra-Urban Heat Exposure in Houston, Texas." *PLoS One* 11, no. 2: e0148890.

Dixon, B., and J. Earls. 2012. "Effects of Urbanization on Streamflow Using SWAT With Real and Simulated Meteorological Data." *Applied Geography* 35, no. 1–2: 174–190.

Dogan, F. N., and M. E. Karpuzcu. 2022. "Effect of Land Use Change on Hydrology of Forested Watersheds." *Ecohydrology* 15, no. 1: e2367.

Dow, C. L., and D. R. DeWalle. 2000. "Trends in Evaporation and Bowen Ratio on Urbanizing Watersheds in Eastern United States." *Water Resources Research* 36: 1835–1843.

Environmental Protection Agency (EPA). 2007. "An Approach for Using Load Duration Curves in the Development of TMDLs." 841-B-07-006.

EPA. 2019. second report on point source progress in hypoxia task force states. https://echo.epa.gov/trends/loading-tool/hypoxia-task-force-nutrient-model.

Epelde, A. M., I. Antiguedad, D. Brito, et al. 2016. "Different Modelling Approaches to Evaluate Nitrogen Transport and Turnover at the Watershed Scale." *Journal of Hydrology* 539: 478–494.

Eshtawi, T., M. Evers, and B. Tischbein. 2016. "Quantifying the Impact of Urban Area Expansion on Groundwater Recharge and Surface Runoff." *Hydrological Sciences Journal* 61, no. 5: 826–843.

Fant, C., R. Srinivasan, B. Boehlert, et al. 2017. "Climate Change Impacts on US Water Quality Using Two Models: HAWQS and US Basins." *Water* 9, no. 2: 118. https://doi.org/10.3390/w9020118.

Ferrant, S., P. Durand, E. Justes, J. L. Probst, and J. M. Sanchez-Perez. 2013. "Simulating the Long Term Impact of Nitrate Mitigation Scenarios in a Pilot Study Basin." *Agricultural Water Management* 124: 85–96.

Gagrani, V., J. A. Diemer, J. J. Karl, and C. J. Allan. 2014. "Assessing the Hydrologic and Water Quality Benefits of a Network of Stormwater Control Measures in a SE US Piedmont Watershed." *JAWRA Journal of the American Water Resources Association* 50, no. 1: 128–142.

Garg, V., B. R. Nikam, P. K. Thakur, S. P. Aggarwal, P. K. Gupta, and S. K. Srivastav. 2019. "Human-Induced Land Use Land Cover Change and Its Impact on Hydrology." *HydroResearch* 1: 48–56.

Gashaw, T., T. Tulu, and M. Argaw. 2019. "Modeling the Impacts of Land Use–Land Cover Changes on Soil Erosion and Sediment Yield in the Andassa Watershed, Upper Blue Nile Basin, Ethiopia." *Environmental Earth Sciences* 78: 679. https://doi.org/10.1007/s12665-019-8726-x.

Ghaffari, G., S. Keesstra, J. Ghodousi, and H. Ahmadi. 2010. "SWAT-Simulated Hydrological Impact of Land-Use Change in the Zanjanrood Basin, Northwest Iran." *Hydrological Processes* 24, no. 7: 892–903.

Glick, R., J. Jeong, R. Srinivasan, J. G. Arnold, and Y. Her. 2023. "Adaptation of SWAT Watershed Model for Stormwater Management in Urban Catchments: Case Study in Austin, Texas." *Water* 15: 1770. https://doi.org/10.3390/w15091770.

Greater Houston Partnership (GHP). 2023. "Fifth Third Bank. 2023 Houston Facts Report."

Harmel, D., S. Potter, P. Casebolt, K. Reckhow, C. Green, and R. Haney. 2006. "Compilation of Measured Nutrient Load Data for Agricultural Land Uses in the United States." *Journal of the American Water Resources Association* 42, no. 5: 1163–1178.

Harmel, D., Q. Song, K. Reckhow, and P. Casebolt. 2008. "The MANAGE Database: Nutrient Load and Site Characteristic Updates and Runoff Concentration Data." *Journal of Quality* 37, no. 6: 2403–2406.

Harmel, R. D., C. W. Richardson, K. W. King, and P. M. Allen. 2006. "Runoff and Soil Loss Relationships for the Texas Blackland Prairies Ecoregion." *Journal of Hydrology* 331, no. 3–4: 471–483.

HAWQS. 2020. "HAWQS System and Data to Model the Lower 48 Conterminous US." Using the SWAT Model, Texas Data Repository Dataverse, V1. https://doi.org/10.18738/T8/XN3TE0.

Homer, C., J. Dewitz, S. Jin, et al. 2020. "Conterminous Land Cover Change Patterns 2001-2016 From the 2016 National Land Cover Database." *ISPRS Journal of Photogrammetry and Remote Sensing* 162: 184–199. https://doi.org/10.1016/j.isprsjprs.2020.02.019.

Houston-Galveston Area Council (H-GAC). 2020. "H-GAC Annual Report."

Hundecha, Y., and A. Bárdossy. 2004. "Modeling of the Effect of Land Use Changes on the Runoff Generation of a River Basin Through Parameter Regionalization of a Watershed Model." *Journal of Hydrology* 292, no. 1–4: 281–295.

Intergovernmental Panel on Climate Change (IPCC). 2014. *Synthesis Report. Contribution of Working Groups I, II and III to the Fifth Assessment Report of the Intergovernmental Panel on Climate Change*, edited by R. K. P. Team and L. A. Meyer, 151. IPCC.

Jeong, J., N. Kannan, J. Arnold, R. Glick, L. Gosselink, and R. Srinivasan. 2010. "Development and Integration of Sub-Hourly Rainfall–Runoff Modeling Capability Within a Watershed Model." *Water Resources Management* 24: 4505–4527.

Johnson, S. L., T. Whiteaker, and D. R. Maidment. 2009. "A Tool for Automated Load Duration Curve Creation 1." *JAWRA Journal of the American Water Resources Association* 45, no. 3: 654–663.

Khan, S. D. 2005. "Urban Development and Flooding in Houston Texas, Inferences from Remote Sensing Data using Neural Network Technique." *Environmental Geology* 47, no. 8: 1120–1127.

Kidane, M., A. Bezie, N. Kesete, and T. Tolessa. 2019. "The Impact of Land Use and Land Cover (LULC) Dynamics on Soil Erosion and Sediment Yield in Ethiopia." *Heliyon* 5, no. 12: e02981.

Kim, H. W., M. H. Li, J. H. Kim, and F. Jaber. 2016. "Examining the Impact of Suburbanization on Surface Runoff Using the SWAT." *International Journal of Environmental Research* 10, no. 3: 379–390.

Knight, R. W., T. L. Thurow, R. K. Heitschmidt, et al. 1995. "Water Yield Improvement From Rangeland Watersheds." Texas Water Development Board, Contract No. lAC (88-89) 0940.

Langner, L. L., L. A. Joyce, and D. N. Wear. 2020. "Future Scenarios: A Technical Document Supporting the USDA Forest Service 2020 RPA Assessment." Gen. Tech. Rep. RMRS-412. Fort Collins, CO: U.S. Department of Agriculture, Forest Service, Rocky Mountain Research Station. 34 p. https://doi.org/10.2737/RMRS-GTR-412.

Lee, T., R. Srinivasan, and N. Omani. 2012. "Estimating the Water Balance of Texas Coastal Watersheds With SWAT. A Case Study of Galveston and Matagorda Bay." A Final Report for the Texas Water Development Board. Project 2009-483-0890.

Li, C., G. Sun, P. V. Caldwell, et al. 2020. "Impacts of Urbanization on Watershed Water Balances Across the Conterminous United States." *Water Resources Research* 56: e2019WR026574.

Lirong, S., and Z. Jianyun. 2012. "Hydrological Response to Climate Change in Beijiang River Basin Based on the SWAT Model." *Procedia Engineering* 28: 241–245.

Moriasi, D. N., J. G. Arnold, M. W. Van Liew, R. L. Bingner, R. D. Harmel, and T. L. Veith. 2007. "Model Evaluation Guidelines for Systematic Quantification of Accuracy in Watershed Simulations." *Journal of the American Society of Agricultural and Biological Engineers* 50: 885–900.

Moriasi, D. N., M. W. Gitau, N. Pai, and P. Daggupati. 2015. "Hydrologic and Water Quality Models: Performance Measures and Evaluation Criteria." *Transactions of the ASABE* 58, no. 6: 1763–1785.

Moriasi, D. N., B. N. Wilson, K. R. Douglas-Mankin, J. G. Arnold, and P. H. Gowda. 2012. "Hydrologic and Water Quality Models: Use, Calibration, and Validation." *Transactions of the ASABE* 55, no. 4: 1241–1247.

Moriasi, D. N., R. W. Zeckoski, J. G. Arnold, et al. 2015. "Hydrologic and Water Quality Models: Key Calibration and Validation Topics." *Transactions of the ASABE* 58, no. 6: 1609–1618.

Moss, R., M. Babiker, and S. Brinkman. 2008. "Towards New Scenarios for Analysis of Emissions, Climate Change, Impacts and Response Strategies. Technical Summary." Geneva, Switzerland: Intergovernmental Panel on Climate Change. 25 p.

Muttiah, R. S., and R. A. Wurbs. 2002. "Modeling the Impacts of Climate Change on Water Supply Reliabilities." *Water International* 27, no. 3: 407–419.

Neitsch, S. L., and J. G. Arnold. 2001. "Soil and Water Assessment Tool Theoretical Documentation Version 2000." http://www.brc.tamus.edu/swat/doc.html.

Neitsch, S. L., J. G. Arnold, J. R. Kiniry, and J. R. Williams. 2005. "Soil and Water Assessment Tool Theoretical Documentation, Version 2005." Grassland, Soil and Water Res. Lab., Agric. Res. Serv., U.S. Dep. Of Agric. Temple, Tex. http://www.brc.tamus.edu/swat/doc.html.

Neitsch, S. L., J. G. Arnold, J. R. Kiniry, and J. R. Williams. 2011. "Soil and Water aAssessment Tool – Theoretical Documentation Version 2009." *Texas Water Resources Institute Technical Report*: 406.

Nelson, E. J., and D. B. Booth. 2002. "Sediment Sources in an Urbanizing, Mixed Land-Use Watershed." *Journal of Hydrology* 264, no. 1–4: 51–68.

Nepal, D., and P. Parajuli. 2024. "Identifying and Assessing Pond Best Management Practice Under Future Climate Scenarios." *Journal of Environmental Management* 370: 122619.

Nguyen, H. H., A. Gericke, and M. Venohr. 2022. "Importance of Different Imperviousness Measures for Predicting Runoff and Nutrient Emissions From Non-Urban and Urban Land-Uses at Large Spatial Coverage." *Journal of Environmental Management* 315: 115105.

O'Driscoll, M., S. Clinton, A. Jefferson, A. Manda, and S. McMillan. 2010. "Urbanizationeffects on Watershed Hydrology and In-Stream Processes in the Southern UnitedStates." *Water* 2, no. 3: 605–648.

Olander, L. P., and B. L. Young. 2016. "Integrating Large-Scale Planning Into Environmental Markets and Related Programs: Status and Trends." Ni WP, 17–03.

Ouyang, Y. 2021. "New Insights on Evapotranspiration and Water Yield in Crop and Forest Lands Under Changing Climate." *Journal of Hydrology* 603: 127192. https://doi.org/10.1016/j.jhydrol.2021.127192.

Ouyang, Y., J. M. Grace, P. B. Parajuli, and P. V. Caldwell. 2022. "Impacts of Multiple Hurricanes and Tropical Storms on Watershed Hydrological Processes in the Florida Panhandle." *Climate* 10, no. 3: 42.

Pai, N., D. Saraswat, and M. Daniels. 2011. "Identifying Priority Subwatersheds in the Illinois River Drainage Area in Arkansas Watershed Using a Distributed Modeling Approach." *Transactions of the ASABE* 54, no. 6: 2181–2196.

Park, Y. S., and B. A. Engel. 2016. "Identifying the Correlation Between Water Quality Data and LOADEST Model Behavior in Annual Sediment Load Estimations." *Water* 8, no. 9: 368.

Paul, M. J., and J. L. Meyer. 2001. "Streams in the Urban Landscape." *Annual Review of Ecology and Systematics* 32, no. 1: 333–365.

PCG. 2019. "PRISM Climate Data." PRISM Climate Group, Northwest Alliance for Computational Science and Engineering, Oregon State University, Corvallis, OR. http://www.prism.oregonstate.edu/.

Pervaiz, F., and A. H. Michelle. 2023. "Effects of Climate Change and Urbanization on Bridge Flood Vulnerability: A Regional Assessment for Harris County, Texas." *Natural Hazards Review* 24, no. 3: e04023025.

Pohlert, T., J. A. Huisman, L. Breuer, and H. G. Frede. 2005. "Modelling of Point and Diffuse Source Pollution of Nitrate With SWAT in the River Dill, Germany." *Advances in Geosciences* 5: 7–12.

PRISM Climate Group. 2023. "PRISM Spatial Climate Datasets for the Coterminous United States." Oregon State University. https://prism.oregonstate.edu/.

Rebich, R. A., N. A. Houston, S. V. Mize, D. K. Pearson, P. B. Ging, and C. Evan Hornig. 2011. "Sources and Delivery of Nutrients to the Northwestern Gulf of Mexico From Streams in the South-Central United States 1." *JAWRA Journal of the American Water Resources Association* 47, no. 5: 1061–1086.

Reitz, M., W. E. Sanford, G. B. Senay, and J. Cazenas. 2017. "Annual Estimates of Recharge, Quick-Flow Runoff,and Evapotranspiration for the Contiguous U.S. Using Empirical Regression Equations." *JAWRA Journal of the American Water Resources Association* 53, no. 4: 961–983. https://doi.org/10.1111/1752-1688.12546.

Reitz, M., G. B. Senay, and W. E. Sanford. 2017. "Combining Remote Sensing and Water-Balance Evapotranspiration Estimates for the Conterminous United States." *Remote Sensing* 9, no. 12: 1181.

Robotham, J., G. Old, P. Rameshwaran, et al. 2023. "Nature-Based Solutions Enhance Sediment and Nutrient Storage in an Agricultural Lowland Catchment." *Earth Surface Processes and Landforms* 48, no. 2: 243–258. https://doi.org/10.1002/esp.5483.

Rose, S., and N. E. Peters. 2001. "Effects of Urbanization on Streamflow in the Atlanta Area (Georgia, USA): A Comparative Hydrological Approach." *Hydrological Processes* 15, no. 8: 1441–1457.

Runkel, R. L., C. G. Crawford, and T. A. Cohn. 2004. "Load Estimator (LOADEST): A Fortran Program for Estimating Constituent Loads in Streams and Rivers." Reston United States Geological Survey.

Russell, K. L., G. J. Vietz, and T. D. Fletcher. 2017. "Global Sediment Yields From Urban and Urbanizing Watersheds." *Earth-Science Reviews* 168: 73–80.

Sajikumar, N., and R. Remya. 2015. "Impact of Land Cover and Land Use Change on Runoff Characteristics." *Journal of Environmental Management* 161: 460–468. https://doi.org/10.1016/j.jenvman.2014.12.041.

Saleh, A., J. G. Arnold, P. W. A. Gassman, et al. 2000. "Application of SWAT for the Upper North Bosque River Watershed." *Transactions of ASAE* 43, no. 5: 1077–1087.

Salerno, F., V. Gaetano, and T. Gianni. 2018. "Urbanization and Climate Change Impacts on Surface Water Quality: Enhancing the Resilience by Reducing Impervious Surfaces." *Water Research* 144: 491–502.

San Jacinto River Authority. 2015. Lake Conroe Watershed Protection Plan. www.sjra.net.

San Jacinto River Authority. 2020. Volumetric and Sedimentation Survey of LAKE CONROE. www.sjra.net.

Sangeetha, K., B. Narasimhan, and R. Srinivasan. 2022. "A Coupled SWAT-AEM Modelling Framework for a Comprehensive Hydrologic Assessment." *Water* 14: 2753. https://doi.org/10.3390/w14172753.

Santhi, C., J. G. Arnold, J. R. Williams, W. A. Dugas, R. Srinivasan, and L. M. Hauck. 2001. "Validation of the Swat Model on a Large Rwer Basin With Point and Nonpoint Sources 1." *JAWRA Journal of the American Water Resources Association* 37, no. 5: 1169–1188.

Scanlon, B., K. Keese, N. Bonal, N. Deeds, V. Kelley, and M. Litvak. 2005. "Evapotranspiration Estimates With Emphasis on Groundwater Evapotranspiration in Texas, Prepared for the Texas Water Development Board."

Schilling, K. E., M. K. Jha, P. W. Zhang, P. Gassman, and C. F. Wolter. 2008. "Impact of Land Use and Land Cover Change on the Water Balance of a Large Agricultural Watershed: Historical Effects and Future Directions." *Water Resources Research* 44: W00A09. https://doi.org/10.1029/2007WR006644.

Shao, M., G. Zhao, S. C. Kao, L. Cuo, C. Rankin, and H. Gao. 2020. "Quantifying the Effects of Urbanization on Floods in a Changing Environment to Promote Water Security—A Case Study of Two Adjacent Basins in Texas." *Journal of Hydrology* 589: 125154.

Shi, P., C. Chen, R. Srinivasan, et al. 2011. "Evaluating the SWAT Model for Hydrological Modeling in the Xixian Watershed and a Comparison With the XAJ Model." *Water Resources Management* 25: 2595–2612.

Shi, P. J., Y. Yuan, J. Zheng, J. A. Wang, Y. Ge, and G. Y. Qiu. 2007. "The Effect of Land Use/Cover Change on Surface Runoff in Shenzhen Region, China." *Catena* 69, no. 1: 31–35.

Shrestha, B., T. A. Cochrane, B. S. Caruso, and M. E. Arias. 2018. "Land Use Change Uncertainty Impacts on Streamflow and Sediment Projections in Areas Undergoing Rapid Development: A Case Study in the Mekong Basin." *Land Degradation & Development* 29, no. 3: 835–848.

Singh, H. V., L. Kalin, A. Morrison, P. Srivastava, G. Lockaby, and S. Pan. 2015. "Post-Validation of SWAT Model in a Coastal Watershed for Predicting Land Use/Cover Change Impacts." *Hydrology Research* 46, no. 6: 837–853.

Sisay, E., A. Halefom, D. Khare, L. Singh, and T. Worku. 2017. "Hydrological Modelling of Ungauged Urban Watershed Using SWAT Model." *Modeling Earth Systems and Environment* 3: 693–702.

Srinivasan, R. 2019. "HAWQS User Guide: Version 1.1." Spatial Sciences Laboratory, Texas A&M AgriLife Research, College Station, TX. https://epahawqs.tamu.edu.

Sui, X., and F. H. van de Ven. 2023. "The Influence of Low Impact Development (LID) on Basin Runoff in a Half-Urbanized Catchment: A Case Study in San Antonio, Texas." *Journal of Hydrology* 616: 128793.

Sun, G., P. Caldwell, A. Noormets, et al. 2011. "Upscaling Key Ecosystem Functions Across the Conterminous United States by a Water-Centric Ecosystem Model." *Journal of Geophysical Research* 116: G00J05. https://doi.org/10.1029/2010JG001573.

Sun, G., P. V. Caldwell, and S. G. McNulty. 2015. "Modelling the Potential Role of Forest Thinning in Maintaining Water Supplies Under a Changing Climate Across the Conterminous United States." *Hydrological Processes* 29, no. 24: 5016–5030.

Suttles, K. M., N. K. Singh, J. M. Vose, et al. 2018. "Assessment of Hydrologic Vulnerability to Urbanization and Climate Change in a Rapidly Changing Watershed in the Southeast US." *Science of the Total Environment* 645: 806–816.

Tang, Z., B. A. Engel, B. C. Pijanowski, and K. J. Lim. 2005. "Forecasting Land Use Change and Its Environmental Impact at a Watershed Scale." *Journal of Environmental Management* 76, no. 1: 35–45.

Texas A&M University. n.d. "Hydrologic and Water Quality System." Accessed on 19 February 2016. https://epahawqs.tamu.edu/.

Texas Natural Resource Conservation Commission; Parsons Engineering Science. 1999. "Report on Surface Water/Groundwater Interaction. Evaluation for 22 Texas River Basins."INC: New York, NY, USA.

Tumsa, B. C., F. F. Feyessa, K. T. Tullu, and A. C. Guder. 2023. "Spatiotemporal Changes of Land Use in Response to Runoff and Sediment Yield for Environmental Sustainability in the Upper Blue Nile Basin, Oromiyaa, Ethiopia." *H2Open Journal* 6, no. 4: 551–575.

Ullrich, A., and M. Volk. 2009. "Application of the Soil and Water Assessment Tool (SWAT) to Predict the Impact of Alternative Management Practices on Water Quality and Quantity." *Agricultural Water Management* 96, no. 8: 1207–1217.

United Nations, Department of Economic and Social Affairs (UN DESA), Population Division. 2019. *World Urbanization Prospects: The 2018 Revision (ST/ESA/SER.A/420)*. United Nations.

United State Environmental Protection Agency (USEPA). 2009. "Environmental Impact and Benefits Assessment for Final Effluent Guidelines and Standards for the Construction and Development Category." Office of Water: Washington, DC, USA, 2009.

United States Department of Agriculture; National Agricultural Statistics Service (NASS). n.d. "Land Use—Cropland Data Layer (Agricultural)." http://nassgeodata.gmu.edu/CropScape/.

United States Geological Survey. n.d. "Land Use (Non-Agricultural)—National Land Cover Database (NLCD)." Accessed on 19 February 2020. http://www.mrlc.gov/nlcd06_data.php.

U.S. Department of Agriculture, Forest Service. 2023. "Future of America's Forest and Rangelands: Forest Service 2020 Resources Planning Act Assessment." Gen. Tech. Rep. WO-102. Washington, DC. 348 p. https://doi.org/10.2737/WO-GTR-102.

USDA-NRCS. 2019. "PRISM. National Water and Climate Center, Natural Resources Conservation Service, U.S. Department of Agriculture: Portland, Oregon." https://www.wcc.nrcs.usda.gov/climate/prism.html.

Vogel, R. M., and N. M. Fennessey. 1995. "Flow Duration Curves II: A Review of Applications in Water Resources Planning 1." *JAWRA Journal of the American Water Resources Association* 31, no. 6: 1029–1039.

Wheater, H., and E. Evans. 2009. "Land Use, Water Management and Future Flood Risk." *Land Use Policy* 26: S251–S264. https://doi.org/10.1016/j.landusepol.2009.08.019.

White, M., M. Gambone, H. Yen, et al. 2016. "Development of a Cropland Management Dataset to Support U.S. Swat Assessments." *JAWRA Journal of the American Water Resources Association* 52, no. 1: 269–274. https://doi.org/10.1111/1752-1688.12384.

White, M., D. Harmel, H. Yen, J. Arnold, M. Gambone, and R. Haney. 2015. "Development of Sediment and Nutrient Export Coefficients for US Ecoregions." *JAWRA Journal of the American Water Resources Association* 51, no. 3: 758–775.

Wilcox, B. P. 2002. "Shrub Control and Streamflow on Rangelands: A Process-Based Viewpoint." *Journal of Range Management* 55: 318–326.

Wilcox, B. P., D. D. Breshears, and M. S. Seyfried. 2003. "Water Balance on Rangelands." In *Encyclopedia of Water Science*, 791–794. Marcel Dekker, Inc.

Wilcox, B. P., L. P. Wilding, and C. M. Woodruff. 2007. "Soil and Topographic Controls on Runoff Generation From Stepped Landforms in the Edwards Plateau of Central Texas." *Geophysical Research Letters* 34: L24S24. https://doi.org/10.1029/2007GL030860.

Williams, H. 2025. "Impact of Urbanization on Rainfall-Runoff Relationships in the Dallas-Fort Worth-Arlington Metropolitan Area, 1990–2020." *Papers in Applied Geography* 11: 1–12.

Woznicki, S. A., P. Cada, J. Wickham, et al. 2020. "Sediment Retention by Natural Landscapes in the Conterminous United States." *Science of the Total Environment* 745: 140972.

Wurbs, R. A. 2021. "Monthly River Flows in Texas for Natural and Developed Conditions." *Water Cycle* 2: 1–14.

Yen, H., P. Daggupati, M. J. White, et al. 2016. "Application of Large-Scale, Multi-Resolution Watershed Modeling Framework Using the Hydrologic and Water Quality System (HAWQS)." *Water* 8, no. 4: 164.

Yen, H., Y. Hoque, R. D. Harmel, and J. Jeong. 2015. "The Impact of Considering Uncertainty in Measured Calibration/Validation Data During Auto-Calibration of Hydrologic and Water Quality Models." *Stochastic Environmental Research and Risk Assessment* 29: 1891–1901.

Zampella, R. A., N. A. Procopio, R. G. Lathrop, and C. L. Dow. 2007. "Relationship of Land-Use/Land-Cover Patterns and Surface-Water Quality in the Mullica River Basin 1." *JAWRA Journal of the American Water Resources Association* 43, no. 3: 594–604.

Zhang, Y., J. Xia, J. Yu, et al. 2018. "Simulation and Assessment of Urbanization Impacts on Runoff Metrics: Insights From Landuse Changes." *Journal of Hydrology* 560: 247–258.

Zhao, G., H. Gao, and L. Cuo. 2016. "Effects of Urbanization and Climate Change on Peak Flows Over the San Antonio River Basin." *Texas. J. Hydrometeorol.* 17, no. 9: 2371–2389. https://doi.org/10.1175/JHM-D-15-0216.1.

Zhu, L., S. M. Quiring, I. Guneralp, and W. G. Peacock. 2015. "Variations in Tropical Cyclone-Related Discharge in Four Watersheds Near Houston, Texas." *Climate Risk Management* 7: 1–10.

Supporting Information

Additional supporting information can be found online in the Supporting Information section. **Data S1:** jawr70083-sup-0001-supinfo.docx.